Side Information Fusion for Recommender Systems over Heterogeneous Information Network

HUAN ZHAO, 4Paradigm Inc., Shenzhen China and Department of Computer Science and Engineering, Hong Kong University of Science and Technology, Hong Kong

QUANMING YAO, 4Paradigm Inc., Hong Kong and Department of Electronic Engineering, Tsinghua University, Beijing, China

YANGQIU SONG, Department of Computer Science and Engineering, Hong Kong University of Science and Technology, Hong Kong

JAMES T. KWOK, Department of Computer Science and Engineering, Hong Kong University of Science and Technology, Hong Kong

DIK LUN LEE, Department of Computer Science and Engineering, Hong Kong University of Science and Technology, Hong Kong

Collaborative filtering (CF) has been one of the most important and popular recommendation methods, which aims at predicting users' preferences (ratings) based on their past behaviors. Recently, various types of side information beyond the explicit ratings users give to items, such as social connections among users and metadata of items, have been introduced into CF and shown to be useful for improving recommendation performance. However, previous works process different types of information separately, thus failing to capture the correlations that might exist across them. To address this problem, in this work, we study the application of heterogeneous information network (HIN), which offers a unifying and flexible representation of different types of side information, to enhance CF-based recommendation methods. However, we face challenging issues in HIN-based recommendation, i.e., how to capture similarities of complex semantics between users and items in a HIN, and how to effectively fuse these similarities to improve final recommendation performance. To address these issues, we apply metagraph to similarity computation and solve the information fusion problem with a "matrix factorization (MF) + factorization machine (FM)" framework. For the MF part, we obtain the user-item similarity matrix from each metagraph and then apply low-rank matrix approximation to obtain latent features for both users and items. For the FM part, we apply FM with Group lasso (FMG) on the features obtained from the MF part to train the recommending model and, at the same time, identify the useful metagraphs. Besides FMG, a two-stage method, we further propose an end-to-end method, hierarchical attention fusing (HAF), to fuse metagraph based similarities for the final recommendation. Experimental results on four large real-world datasets show that the two proposed frameworks significantly outperform existing state-of-the-art methods in terms of recommendation performance.

1 INTRODUCTION

In the big data era, people are overwhelmed by the huge amount of information on the Internet, making recommender systems (RSs) an indispensable tool for getting interesting information. Collaborative filtering (CF) has been the most popular recommendation method in the last decade [Herlocker et al. 1999; Koren 2008], which tries to predict a user's preferences based on their past behaviors. In recent years, researchers try to incorporate auxiliary information beyond users' behaviors, or *side information*, to enhance CF. For example, social connections among users [Ma et al. 2011; Xiao et al. 2019; Zhao et al. 2017a], reviews of items [Ling et al. 2014; McAuley and Leskovec 2013], metadata attached to commodities [Wang et al. 2018], or locations of users and items [Ye et al. 2011; Zheng et al. 2012], have been shown to be effective for improving recommendation performance. However, a major limitation of most existing methods is that various types of side information are processed independently, leading to information loss across different types of side information. This limitation becomes more and more severe, because modern websites record rich side information about their users and contents [Pan 2016] and it would be a huge loss to their business if the side information cannot be fully utilized to improve performance. For example, on Yelp (https://www.yelp.com/), a website recommendation business to users, users can follow other users to form a social network, businesses have categories and locations, and users can write reviews on businesses. If each type of side information is processed in isolation, information that exists across different types of side information will be neglected. Therefore, a unifying framework is needed to fuse all side information for producing effective recommendations.

Heterogeneous information networks (HINs) [Shi et al. 2017; Sun et al. 2011] have been proposed as a general data representation tool for different types of information, such as scholar network [Sun et al. 2011] and knowledge graph [Wang et al. 2015a]. Thus, by modeling various side information and the relations between them as different nodes (entities) and edges, respectively, HIN can be used as a unifying framework for RSs [Shi et al. 2015; Yu et al. 2014]. Figure 1 shows an example HIN on Yelp, and Figure 2 shows a network schema defined over the entity types *User*, *Review*, *Aspect*, *Business*, etc. Based on the network schema, we can design metapaths [Shi et al. 2017; Sun et al. 2011], which are sequences of node types, to compute the similarities between users and businesses for generating recommendations. For example, we can define complicated metapaths such as *User → Review → Aspect → Review → User → Business*, to measure similarities between user and business based on similar reviews written by users about the same aspect. Therefore, we can unify different side information with HIN and design metapaths to compute user-item similarities of different semantics for making more effective recommendation.

However, there are **two major issues** facing existing HIN-based RSs. The first issue is that metapaths are not enough for representing the rich semantics for HIN-based RSs. We refer to it as *semantic limitation*. Figure 1 shows a concrete example, where the metapath *User → Review → Aspect → Review → User → Business* is used to capture users' similarity since both users write reviews and mention the same aspect (seafood) in the review texts. However, if we want to capture the similarity induced by the two users' reviews mentioning the same aspect (such as *seafood*) and ratings on the same business (such as *Royal House*), then metapath is not able to capture this semantic. Thus, we need a better way to capture such complicated semantics. Recently, Huang et al.
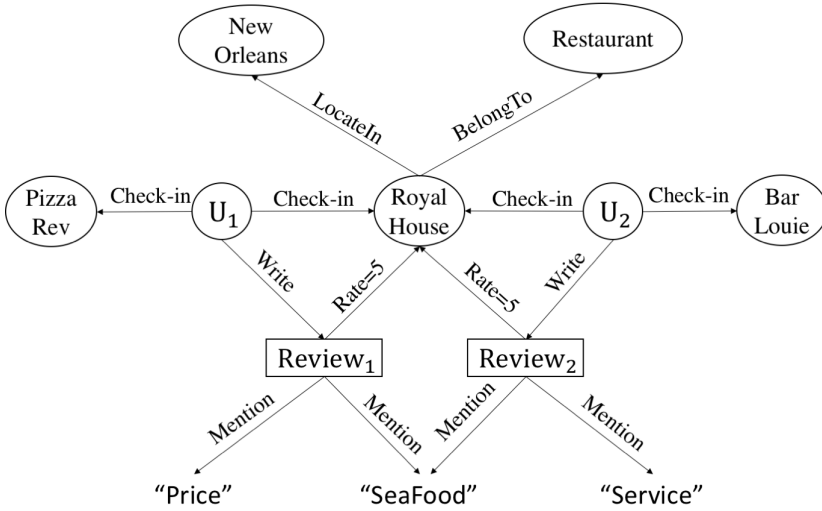
Fig. 1. An example HIN built for Royal House on Yelp. We can see that various side information, like Category (Restaurant) and City (New Orleans), are modeled as nodes (entities) of different types. And the corresponding relations among different side information are modeled by edges.

[2016] and Fang et al. [2019, 2016] proposed to use metagraph (or meta-structure) for computing similarity between homogeneous types of entities (e.g., using *Person* to search *Person*) over HINs, which is more powerful than metapath in capturing complex semantics. However, they did not explore metagraphs for entities of heterogeneous types, which are essential for RSs. In this paper, we extend metagraph to capture similarities of complex semantics between users and items (businesses) in recommendation scenarios.

The second issue is about *similarity fusion*, i.e., how to fuse the similarities of different semantics between users and items for recommendation. Our goal is to achieve accurate predictions of the users' ratings given these similarities. In general, there are three groups of approaches to do so. The first ones are directly using the metapath based similarity to improve the rating prediction task. For example, in [Shi et al. 2015], the proposed method firstly computes multiple similarity matrices between users and items based on different metapaths, and then learn a weighted mechanism to explicitly combine these similarities to approximate the user-item rating matrix. However, these similarity matrices could be too sparse to contribute to the final ensemble. The second ones are to firstly factorize each user-item similarity matrix to obtain user and item latent features, and then use all latent features to recover the user-item rating matrix [Shi et al. 2018; Yu et al. 2014]. These methods solve the sparsity problem associated with each similarity matrix. However, it does not fully utilize the latent features because they ignore the latent feature interactions among different metapaths and only capture linear interactions among the latent features. The third group of approaches are similar to the second ones, while they propose to use neural network based methods to extract and fuse latent features in an end-to-end manner [Fan et al. 2019; Hu et al. 2018; Jin et al. 2020]. However, all these methods still rely on metapath, thus failing to capture complex semantics. In one words, existing HIN-based recommendation methods [Fan et al. 2019; Hu et al. 2018; Jin et al. 2020; Shi et al. 2015; Yu et al. 2014] suffer from information loss in various ways.

To address the above challenges, we propose a new systematic way to fuse various side information in HIN for recommendation. First, instead of using metapath for recommendation [Shi
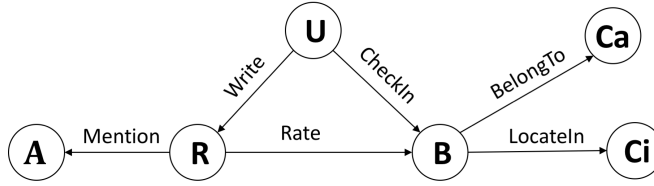
Fig. 2. The network schema for the HIN in Figure 1. A: aspect extracted from reviews; R: reviews; U: users; B: business; Cat: category of business; Ci: city.

et al. 2015; Yu et al. 2014], we introduce the concept of metagraph to the recommendation problem, which allows us to incorporate more complex semantics into HIN-based RSs. Second, instead of computing the recovered matrices directly from the metagraphs, we utilize the latent features from all metagraphs. Based on matrix factorization (MF) [Koren 2008; Mnih and Salakhutdinov 2007] and factorization machine (FM) [Rendle 2012], we propose a "MF + FM" framework for our metagraph based RS in HIN. We first compute the user-item similarity matrix from each metagraph and then factorize the similarity matrix to obtain a set of vectors representing the latent features of users and items. Finally, we use FM to assemble these latent features to predict the missing ratings that users give to the items. This method enables us to capture nonlinear interactions among all latent features, which has been demonstrated to be effective in FM-based RS [Rendle 2012]. To further improve the performance of the "MF+FM" framework, we propose to use group lasso [Jacob et al. 2009] with FM (denote as FMG) to learn the parameters for selecting metagraphs that contribute most to the recommendation performance. As a result, we can automatically determine which metagraphs are the most effective, and for each group of user and item features from a metagraph, how the features should be weighed. Besides FMG, a two-stage method to extract and fuse latent features from multiple metagraph based user-item similarities, we further propose a novel method based on graph neural networks (GNN) [Battaglia et al. 2018], i.e., the hierarchical attention fusion (HAF) framework, which can fuse multiple metagraph based user-item similarities in an end-to-end manner. Experimental results on four large real-world datasets, Amazon and Yelp, show that our frameworks significantly outperform recommendation methods that are solely based on MF, FM, or metapath in HIN. Our code is available at https://github.com/HKUST-KnowComp/FMG.

Preliminary results of this manuscript have been reported in KDD 2017 [Zhao et al. 2017b], where MF is designed to extract latent features from metagraphs, and then FMG is proposed for metagraph fusion and selection. In this manuscript, we formally propose and highlight the systematic framework "MF + FM" (see Figure 3), which provides a complete solution for HIN-based RSs. Compared to the KDD version, we update the three key components of FMG by designing a novel latent feature extraction method for the MF part, a novel type of group lasso regularizer, and a more efficient optimization solver for the FM part, respectively. Moreover, we further propose the HAF framework (see Figure 6), which can be regarded as a deep learning version of "MF + FM" pipeline, benefited from the advantages of neural networks and end-to-end training. Finally, additional experiments are performed to support the newly introduced components.

Notation

We denote vectors and matrices by lowercase and uppercase boldface letters, respectively. In this paper, a vector always denote row vector. For a vector $\mathbf{x}$, $\|\mathbf{x}\|_2 = (\sum_{i=1} |\mathbf{x}_i|^2)^{\frac{1}{2}}$ is its ℓ_2-norm. For a matrix $\mathbf{X}$, its nuclear norm is $\|\mathbf{X}\|_* = \sum_i \sigma_i(\mathbf{X})$, where $\sigma_i(\mathbf{X})$'s are the singular values of $\mathbf{X}$; $\|\mathbf{X}\|_F = (\sum_{i,j} \mathbf{X}_{ij}^2)^{\frac{1}{2}}$ is its Frobenius norm and $\|\mathbf{X}\|_1 = \sum_{i,j} |\mathbf{X}_{ij}|$ is its ℓ_1-norm. For two matrices $\mathbf{X}$

and Y, $\langle X, Y \rangle = \sum_{i,j} X_{ij} Y_{ij}$, and $[X \odot Y]_{ij} = X_{ij} Y_{ij}$ denotes the element-wise multiplication. For a smooth function f, $\nabla f(\mathbf{x})$ is its gradient at $\mathbf{x}$.

2 RELATED WORK

In this section, we review existing works related to HIN, RS with various side information, and RS over HIN.

2.1 Heterogeneous Information Networks (HINs)

HINs have been proposed as a general representation for many multi-typed objects and multi-relational interactions among these objects, which are often modeled as graphs or networks [Dong et al. 2017, 2020; Kong et al. 2013b; Shi et al. 2017; Sun and Han 2013; Sun et al. 2011; Yang et al. 2020]. To capture rich semantics underlying HINs, metapath, a sequence of entity types defined by the HIN network schema, has played a key role in modeling similarities between nodes. Based on metapath, several similarity measures, such as PathCount [Sun et al. 2011], PathSim [Sun et al. 2011], and PCRW [Lao and Cohen 2010] have been proposed, and research has shown that they are useful for entity search and as similarity measure in many real-world networks. After the development of metapath, many data mining tasks have been enabled or enhanced, including recommendation [Fan et al. 2019; Hu et al. 2018; Jin et al. 2020; Shi et al. 2015; Yu et al. 2013, 2014], similarity search [Shi et al. 2014; Sun et al. 2011], clustering [Sun et al. 2013; Wang et al. 2015a], classification [He et al. 2019; Jiang et al. 2017; Kong et al. 2013a; Wang et al. 2017, 2015b], link prediction [Sun et al. 2012; Zhang et al. 2014], malware detection [Fan et al. 2018a; Hou et al. 2017], and opioid user detection [Fan et al. 2018b]. Recently, metagraph (or meta-structure) has been proposed for capturing complicated semantics in HIN that metapath cannot handle [Fang et al. 2019, 2016; Huang et al. 2016; Yang et al. 2018; Zhang et al. 2018, 2020; Zhao et al. 2019].

2.2 Recommendation with Side Information

Modern recommender systems are able to capture rich side information such as social connections among users and metadata and reviews associated with items. Previous works have explored different methods to incorporate heterogeneous side information to enhance CF based recommender systems. For example, Ma et al. [2011] and Zhao et al. [2017a], respectively, incorporate social relations into low-rank and local low-rank matrix factorization to improve the recommendation performance, and heterogeneous item relations are explored for recommendation in [Kang et al. 2018]. Ye et al. [2011] proposed a probabilistic model to incorporate users' preferences, social network and geographical information to enhance point-of-interests recommendation. In [Wang et al. 2019c], knowledge graph is used to enhance the item representation in textual content recommendation. In [Xiao et al. 2019, 2020], social connections and textual features are processed together in a graph attention network framework for content recommendation. Zheng et al. [2012] proposed to integrate users' location data with historical data to improve the performance of point-of-interest recommendation. Pfadler et al. [2020]; Wang et al. [2018] proposed embedding based methods to incorporate side informations of commodities to improve the recommendation performance of e-commerce systems. These previous approaches have demonstrated the importance and effectiveness of heterogeneous side information in improving recommendation accuracy. However, most of these approaches deal with these side information separately, hence losing important information that might exist across them.

2.3 Recommendation over Heterogeneous Information Networks

HIN-based recommendation has been proposed to avoid the disparate treatment of different types of information. Based on metapath, user-item similarities of different semantics can be captured,

based on which extensive methods have been proposed. In general, these methods can be roughly categorized into three groups. The first ones are to use metapath based similarities *explicitly*, either as supervision signals or features. In [Yu et al. 2013], metapath based similarities are used as regularization terms in matrix factorization. In [Shi et al. 2015], a linear combination prediction method is used to fuse multiple metapath based similarities for rating prediction. The second group of methods use metapath based similarities *implicitly*, which firstly obtain latent features of users and items from these user-item similarities, and different prediction models are designed on user and item latent features. In [Yu et al. 2014], multiple metapaths are used to learn user and item latent features, which are then used to recover similarity matrices combined by a weighted mechanism. In the KDD version of this manuscript [Zhao et al. 2017b], our FMG framework falls into this group, where MF is used to extract latent features, while FM is used to predict by these latent features. In [Shi et al. 2018], metapath based embedding is utilized firstly and several fusion functions are designed to fuse these metapath based embeddings, i.e., latent features of users and items. The third group of methods are to employ recently popular neural models to fuse metapath based features or similarities. In [Shi et al. 2019], a neural attention model is designed to extract and fuse latent features from metapath based similarities between users and items for the top-N recommendation. In [Hu et al. 2018], metapath instances are treated as context for recommendation, and a co-attention model is proposed to extract and fuse user, item, and metapath contexts for the final recommendation. In [Fan et al. 2019], metapath is used to select neighbors, which are incorporated into the popular message passing GNN models for e-commerce recommendation. Further, in [Jin et al. 2020], metapath based neighborhood is defined formally, and an efficient neighborhood interaction neural model is designed to fuse user-item interactions in a more fine-grained way.

However, all these three groups of methods rely on metapath for HIN-based RS, except our FMG, thus failing to capture the complex semantics by metagraph. Besides the "MF + FM" framework, we further design the HAF framework, which falls in the third group, to perform the fusion and selection for all metagraph based features in an end-to-end manner. Note that despite the end-to-end training nature, conceptually, the third group of methods can still be seen as a special case of the designed pipeline in Figure 3, since they all follow an embedding (feature extraction) + multilayer perceptron (MLP) (feature fusion) pipeline, which is a standard practice in existing neural models nowadays.

3 "MF + FM" FRAMEWORK

The proposed "MF + FM" framework is illustrated in Figure 3. The input to the MF part is a HIN, e.g., the one in Figure 1. To solve the semantic limitation issue, we propose to use metagraph instead of metapath to capture complex semantics that exists between users and items in a HIN, e.g., those in Figure 4 and 5. Let there be L metagraphs. The MF part, introduced in Section 4, computes from the L metagraphs L user-item similarity matrices, denoted by $\mathbf{R}^1, \mathbf{R}^2, \cdots, \mathbf{R}^L$. We then apply low-rank matrix approximation to factorize each similarity matrix into two low-dimensional matrices, representing the latent features of users and items, which is also a classical method in CF based recommendation [Koren 2008]. The output of the MF part is the L groups of latent features for users and items. Since existing methods only compute metapath based similarities, we design a new algorithm to compute metagraph based user-item similarities.

The objective of the FM part is to utilize the latent features to learn a recommendation model that is more effective than previous HIN-based RSs. This addresses the similarity fusion issue. FMG (see Section 5) has two advantages over previous methods: 1) FM can capture non-linear interactions among features [Rendle 2012], and thus more effective than linear ensemble model adopted in previous HIN-based RS [Yu et al. 2014], 2) by introducing group lasso regularization, we

Fig. 3. The proposed "MF + FM" framework. In the MF part, latent features are extracted from user–item similarity matrices derived from metagraphs in a HIN (e.g., Figure 1). In the FM part, latent features are concatenated and then fed into FMG to predict missing ratings. In the bottom, the features in grey are selected by group lasso regularizers.

can automatically select the useful features and in turn the useful metagraphs for a recommendation application, avoiding laborious feature and metagraph engineering when a new HIN is encountered. Specifically, for a user-item pair, user u_i and item b_j, we first concatenate the latent features $\mathbf{u}_i^1, \mathbf{u}_i^2, \cdots, \mathbf{u}_i^L$ and $\mathbf{b}_i^1, \mathbf{b}_i^2, \cdots, \mathbf{b}_i^L$ from all of the metagraphs to create a feature vector, using rating $\mathbf{R}_{ij}$ as label. We then train our FMG model with group lasso regularization method to select the useful features in the groups, where each group corresponds to one metagraph. The selected features are in grey in Figure 3. Finally, to efficiently train FMG, we propose two algorithms, one is based on the proximal gradient algorithm [Parikh and Boyd 2014] and the other on the stochastic variance reduced gradient algorithm [Xiao and Zhang 2014] (see Section 5.3).

Note that FMG follows a two-stage pipeline, where the feature extraction and fusion are trained separately. Motivated by the recent success of neural network methods in various domains, we further design a hierarchical attention framework (see Figure 6) based on graph neural network models, which integrates these two stages and can be trained in an end-to-end manner. In Section 7.2,

we can see that HAF outperforms FMG by a large margin, which demonstrates the power of neural network models.

Remark 3.1. The main contribution of this paper is the novel and systematical paradigm to fuse different types of side information over HIN for the popular CF based recommendation problems. This paradigm includes two types of frameworks: one is the "MF + FM" framework in Figure 3, and the other is the neural framework in Figure 6. Despite the effectiveness of these two frameworks, another problem is facing all HIN-based recommendation methods in practice, which is that *how to construct a HIN in a recommendation scenario*. In the context of the rating prediction task in CF based recommendation, we refer to *any potentially useful auxiliary information* beyond the rating matrix as side information, e.g., the social connections among users, meta-data of items, and reviews including texts and images. In general, those in discrete values, e.g., category, city, state in Figure 1, can be directly modeled as nodes in a HIN, however, there are some types of side information which cannot be easily to modeled in a HIN. For example, to make use of the textual content of reviews in Yelp (Figure 1), we extract keywords from each review as *Aspect* node in a HIN by natural language processing techniques (see the network schema in Figure 2), however, it remains to be a challenging and unknown problem to incorporate images into the constructed HIN. This problem can be a potential future direction beyond this work, not only in recommendation scenarios, but also in other HIN-based problems, e.g., intent recommendation [Fan et al. 2019], fraud detection [Hu et al. 2019], malware detection in software systems [Fan et al. 2018a; Hou et al. 2017]. Once a HIN is constructed, the proposed methods in this paper can naturally be adopted, which demonstrates the practical values in broader domains.

4 METAGRAPH CONSTRUCTION AND FEATURE EXTRACTION

In this section, we elaborate on the MF part for metagraph based feature extraction. In Section 4.1, we introduce the method for constructing metagraphs in HIN. Then, we show how to compute the user-item similarity matrices in Section 4.2. Finally, in Section 4.3, we obtain latent features from the user-item matrices using MF-based approaches. The main novelty of our approach is the design of the MF part, which extracts and combines latent features from each metagraph before they are fed to the FM part. Further, as existing methods are only for computing similarity matrices based on metapath, we show how similarity can be computed for metagraph.

4.1 Construction of Metagraphs

We first give the definitions of HIN, network schema for HIN, and Metagraph [Fang et al. 2019, 2016; Huang et al. 2016; Sun et al. 2011]. Then, we introduce how to compute metagraph based similarities between users and items in a HIN.

Definition 1 (Heterogeneous Information Network). A **heterogeneous information network** (HIN) is a graph $\mathcal{G} = (\mathcal{V}, \mathcal{E})$ with an entity type mapping $\phi \colon \mathcal{V} \to \mathcal{A}$ and a relation type mapping $\psi \colon \mathcal{E} \to \mathcal{R}$, where $\mathcal{V}$ denotes the entity set, $\mathcal{E}$ denotes the link set, $\mathcal{A}$ denotes the entity type set, and $\mathcal{R}$ denotes the relation type set, and the number of entity types $|\mathcal{A}| > 1$ or the number of relation types $|\mathcal{R}| > 1$.

Definition 2 (Network schema). Given a HIN $\mathcal{G} = (\mathcal{V}, \mathcal{E})$ with the entity type mapping $\phi \colon \mathcal{V} \to \mathcal{A}$ and the relation type mapping $\psi \colon \mathcal{E} \to \mathcal{R}$, the **network schema** for network $\mathcal{G}$, denoted by $\mathcal{T}_{\mathcal{G}} = (\mathcal{A}, \mathcal{R})$, is a graph, in which nodes are entity types from $\mathcal{A}$ and edges are relation types from $\mathcal{R}$.

Figures 1 and 2 show an example of HIN and its network schema from the Yelp dataset respectively. We can see that we have different types of nodes, e.g., *User, Review, Restaurant*, and different types
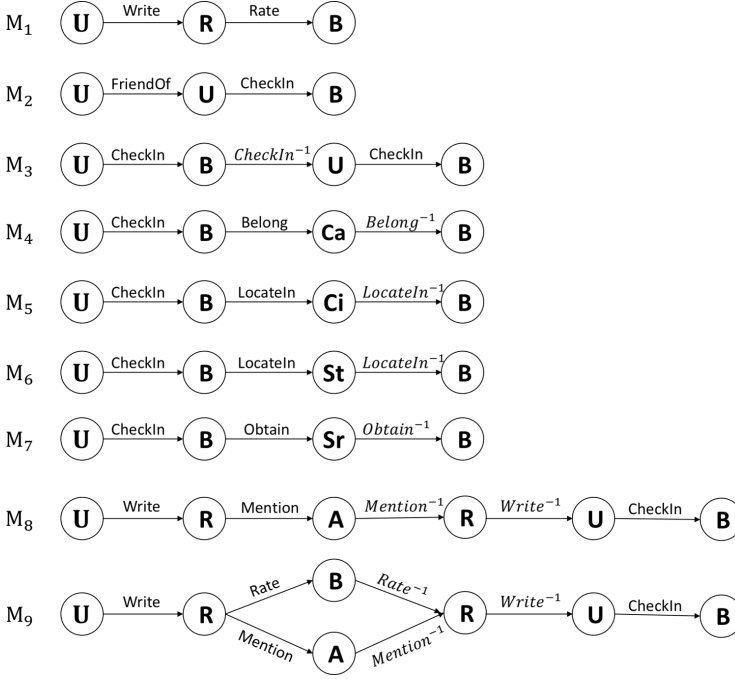
Fig. 4. Metagraphs used for the Yelp dataset (**Ca**: Category; **Ci**: City; **St**: State; **Sr**: Star, the average number of stars a business obtained).

of relations, e.g., *Write* and *CheckIn*. The network schema defines the relations between node types, e.g., *User CheckIn Restaurant*, and *Restaurant LocateIn City*. Thus, we can see that HIN is a flexible way for representing various information in a unified manner. The definition of metagraph is given below.

Definition 3 (Metagraph). A metagraph $\mathcal{M}$ is a directed acyclic graph (DAG) with a single source node n_s (i.e., with in-degree 0) and a single sink (target) node n_t (i.e., with out-degree 0), defined in a HIN $\mathcal{G} = (\mathcal{V}, \mathcal{E})$. Formally, $\mathcal{M} = (\mathcal{V}_M, \mathcal{E}_M, \mathcal{A}_M, \mathcal{R}_M, n_s, n_t)$, where $\mathcal{V}_M \subseteq \mathcal{V}$ and $\mathcal{E}_M \subseteq \mathcal{E}$ are constrained by $\mathcal{A}_M \subseteq \mathcal{A}$ and $\mathcal{R}_M \subseteq \mathcal{R}$, respectively.

As in [Fang et al. 2019, 2016; Huang et al. 2016], compared to metapath, metagraph can capture more complex semantics underlying the similarities between users and items. In fact, metapath is a special case of metagraph. Thus, in this paper, we introduce the concept of metagraph for HIN-based RS. In Figures 4 and 5, we show the metagraphs on Yelp and Amazon datasets, respectively, used in our experiments. In these figures, $\mathcal{R}^{-1}$ represents the reverse relation of $\mathcal{R}$. For example, for M_3 in Figure 4, $B \xrightarrow{CheckIn^{-1}} U$ means U checks in a business B. From Figure 4 and 5, we can see that each metagraph has only one source (U) and one target (B) node, representing a user and an item in the recommendation scenario.

4.1.1 Practical Suggestions. Since there could be many metagraphs in a HIN and they are not equally effective, we give three guidelines for the selection of metagraphs: 1) All metagraphs designed are from the network schema. 2) Domain knowledge is helpful because some metagraphs correspond to traditional recommendation strategies that have been proven to be effective [Shi et al. 2015; Yu et al. 2014]. For example, $\mathcal{M}_2$ and $\mathcal{M}_3$ in Figure 4, respectively, represent social
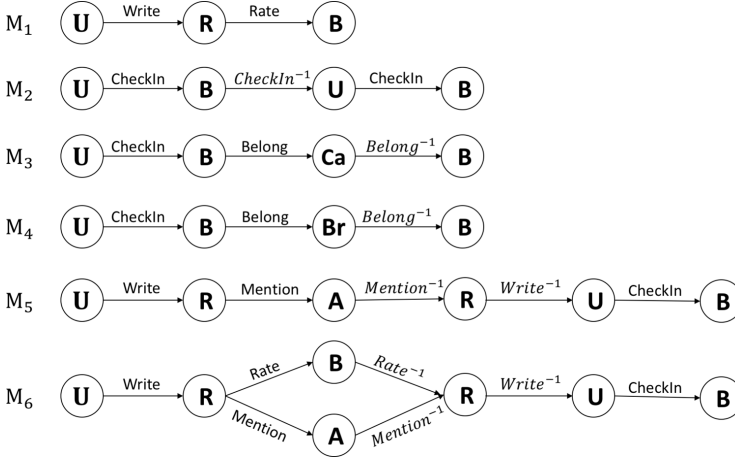
Fig. 5. Metagraphs used for the Amazon dataset (Ca: Category; Br: Brand of the item).

recommendation and the well-known user-based CF. In practice, an understanding of existing recommendation strategies and application semantics is essential for the design of good metagraphs; 3) It is better to construct shorter metagraphs. In [Sun et al. 2011], the authors have shown that longer metapaths decrease the performance because they tend to have more noises. This result is applicable to metagraphs as well.

4.2 Computation of Similarity Matrices

We use $\mathcal{M}_3$ and $\mathcal{M}_9$ in Figure 4 to illustrate the computation of metagraph based similarities. In previous works, commuting matrices [Sun et al. 2011] have been employed to compute the count-based similarity matrix of a metapath. Suppose we have a metapath $\mathcal{P} = (\mathbb{A}_1, \mathbb{A}_2, \ldots, \mathbb{A}_l)$, where $\mathbb{A}_i$'s are node types in $\mathcal{A}$ and denote the adjacency matrix between type $\mathbb{A}_i$ and type $\mathbb{A}_j$ by $\mathbf{W}_{\mathbb{A}_i \mathbb{A}_j}$. Then the commuting matrix for $\mathcal{P}$ is defined by the multiplication of a sequence of adjacency matrices:

$$\mathbf{C}_P = \mathbf{W}_{\mathbb{A}_1, \mathbb{A}_2} \mathbf{W}_{\mathbb{A}_2, \mathbb{A}_3} \cdots \mathbf{W}_{\mathbb{A}_{l-1}, \mathbb{A}_l},$$

where $\mathbf{C}_P(i, j)$, the entry in the i-th row and j-th column, represents the number of path instances between object $x_i \in \mathbb{A}_1$ and object $x_j \in \mathbb{A}_l$ under $\mathcal{P}$. For example, for $\mathcal{M}_3$ in Figure 4, $\mathbf{C}_{M_3} = \mathbf{W}_{UB} \mathbf{W}_{UB}^\top \mathbf{W}_{UB}$, where $\mathbf{W}_{UB}$ is the adjacency matrix between type U and type B, and $\mathbf{C}_{M_3}(i, j)$ represents the number of instances of $\mathcal{M}_3$ between user u_i and item b_j. In this paper, for a metagraph $\mathcal{M}$, the similarity between a source object and a target object is defined as the number of instances of $\mathcal{M}$ connecting the source and target objects. In the remainder of this paper, we adopt the term similarity matrix instead of commuting matrix for clarity.

From the above introduction, we can see that metapath based similarity matrix is easy to compute. However, for metagraphs, the problem is more complicated. For example, consider $\mathcal{M}_9$ in Figure 4, there are two ways to pass through the metagraph, which are (U, R, A, R, U, B) and (U, R, B, R, U, B). Note that R represents the entity type *Review* in HIN. In the path (U, R, A, R, U, B), (R, A, R) means if two reviews mention the same A (*Aspect*), then they have some similarity. Similarly, in (U, R, B, R, U, B), (R, B, R) means if two reviews rate the same B (*Business*), they have some similarity too. We should decide how similarity should be defined when there are multiple ways to pass through the metagraph from the source node to the target node. We can require a flow to pass through either path or both paths in order to be considered in similarity computation. The

former strategy simply splits a metagraph into multiple metapaths, thus suffering from information loss. Therefore, we adopt the latter, but it requires one more matrix operation in addition to simple multiplication, i.e, element-wise product. Algorithm 1 depicts the algorithm for computing count-based similarity based on $\mathcal{M}_9$ in Figure 4. After obtaining $\mathbf{C}_{S_r}$, we can get the whole similarity matrix $\mathbf{C}_{M_9}$ by multiplying the sequence of matrices along $\mathbf{C}_{M_9}$. In practice, not limited to $\mathcal{M}_9$ in Figure 4, the metagraph defined in this paper can be computed by two operations (Hadamard product and multiplication) on the corresponding matrices.

Algorithm 1 Computing similarity matrix based on $\mathcal{M}_9$.

1: Compute $\mathbf{C}_{P_1}$: $\mathbf{C}_{P_1} = \mathbf{W}_{RB}\mathbf{W}_{RB}^\top$;
2: Compute $\mathbf{C}_{P_2}$: $\mathbf{C}_{P_2} = \mathbf{W}_{RA}\mathbf{W}_{RA}^\top$;
3: Compute $\mathbf{C}_{S_r}$: $\mathbf{C}_{S_r} = \mathbf{C}_{P_1} \odot \mathbf{C}_{P_2}$;
4: Compute $\mathbf{C}_{M_9}$: $\mathbf{C}_{M_9} = \mathbf{W}_{UR}\mathbf{C}_{S_r}\mathbf{W}_{UR}^\top\mathbf{W}_{UB}$.

By computing the similarities between all users and items for the l-th metagraph $\mathcal{M}$, we can obtain a user-item similarity matrix $\mathbf{R}^l \in \mathbb{R}^{m \times n}$, where $\mathbf{R}^l_{ij}$ represents the similarity between user u_i and item b_j along the metagraph, and m and n are the number of users and items, respectively. Note that $\mathbf{R}^l_{ij} = \mathbf{C}_{M_l}(i, j)$ [1] if $\mathbf{C}_{M_l}(i, j) > 0$ and 0 otherwise. By designing L metagraphs, we can get L different user-item similarity matrices, denoted by $\mathbf{R}^1, \ldots, \mathbf{R}^L$.

4.3 Latent Feature Generation

In this part, we elaborate on how to generate latent features for users and items from the L user-item similarity matrices. Since the similarity matrices are usually very sparse, using the matrices directly as features will lead to the high-dimensional learning problem, resulting in overfitting. Motivated by the success of low-rank matrix completion [Candès and Recht 2009; Koren 2008; Mnih and Salakhutdinov 2007], we propose to generate latent features using these methods.

Specifically, the nonzero elements in a similarity matrix are treated as observations and the others are taken as missing values. Then we find a low-rank approximation to this matrix. Matrix factorization (MF) [Koren 2008; Mnih and Salakhutdinov 2007] and nuclear norm regularization (NNR) [Candès and Recht 2009] are two popular approaches for matrix completion. Generally, MF leads to nonconvex optimization problems, while NNR leads to convex optimization problems. NNR is easier to optimize and has better theoretical guarantee on the recovery performance than MF. Empirically, NNR usually has better performance and the recovered rank is often much higher than that of MF [Yao and Kwok 2015]. In this paper, we generate metagraph based latent features with both methods and conduct experiments to compare their performance (shown in Section 7.4.1). The technical details of these two methods are introduced in the remaining part of this section.

4.3.1 Matrix Factorization. Consider a user-item similarity matrix $\mathbf{R} \in \mathcal{R}^{m \times n}$, let the observed positions be indicated by 1's in $\Omega \in \{0, 1\}^{m \times n}$, i.e., $[P_\Omega(\mathbf{X})]_{ij} = \mathbf{X}_{ij}$ if $\Omega_{ij} = 1$ and 0 otherwise. $\mathbf{R}$ is factorized as a product of $\mathbf{U} \in \mathcal{R}^{m \times F}$ and $\mathbf{B} \in \mathcal{R}^{n \times F}$ by solving the following optimization problem:

$$\min_{\mathbf{U},\mathbf{B}} \frac{1}{2} \left\| P_\Omega \left(\mathbf{U}\mathbf{B}^\top - \mathbf{R} \right) \right\|_F^2 + \frac{\mu}{2} \left(\|\mathbf{U}\|_F^2 + \|\mathbf{B}\|_F^2 \right), \tag{1}$$

where $F \ll \min(m, n)$ is the desired rank of $\mathbf{R}$, and μ is the hyper-parameter controlling regularization.

---

[1] To maintain consistency with the remaining sections, we change the notation $\mathbf{C}$ into $\mathbf{R}$.

We adopt the gradient descent based approach for optimizing (1), which is popular in RSs [Koren 2008; Mnih and Salakhutdinov 2007]. After optimization, we take $\mathbf{U}$ and $\mathbf{B}$ as the latent features of users and items, respectively.

4.3.2 Nuclear Norm Regularization. Although MF can be simple, (1) is not a convex optimization problem, so there is no rigorous guarantee on the recovery performance. This motivates our adoption of nuclear norm, which is defined as the sum of all singular values of a matrix. It is also the tightest convex envelope to the rank function. This leads to the following nuclear norm regularization (NNR) problem:

$$\min_{\mathbf{X}} \frac{1}{2} \left\| P_\Omega(\mathbf{X} - \mathbf{R}) \right\|_F^2 + \mu \left\| \mathbf{X} \right\|_*, \tag{2}$$

where $\mathbf{X}$ is the low-rank matrix to be recovered, and μ is the hyper-parameter controlling regularization. Nice theoretical guarantee has been developed for (2), which shows that $\mathbf{X}$ can be exactly recovered given sufficient observations [Candès and Recht 2009]. These advantages make NNR popular for low-rank matrix approximation [Candès and Recht 2009]. Thus, we adopt (2) to generate latent features, using the state-of-the-art AIS-Impute algorithm [Yao and Kwok 2015] in optimizing (2). It has fast $O(1/T^2)$ convergence rate, where T is the number of iterations, with low per-iteration time complexity. In the iterations, a Singular Value Decomposition (SVD) of $\mathbf{X} = \mathbf{P}\Sigma\mathbf{Q}^\top$ is maintained (Σ only contains the nonzero singular values). When the algorithm stops, we take $\mathbf{U} = \mathbf{P}\Sigma^{\frac{1}{2}}$ and $\mathbf{B} = \mathbf{Q}\Sigma^{\frac{1}{2}}$ as user and item latent features, respectively.

4.4 Complexity Analysis

We analyze the time complexity of the MF part, which includes similarity matrix computation and latent feature generation. For similarity matrix computation, the core part is matrix multiplication. Since the adjacency matrices tend to be very sparse, they can be implemented very efficiently as sparse matrices. Moreover, for MF and NNR, according to [Yao and Kwok 2015; Yao et al. 2018], the computation cost in each iteration is $O(\|\Omega\|_1 F + (m+n)F)$ and $O(\|\Omega\|_1 F + (m+n)F^2)$, respectively, where $\|\Omega\|_1$ is the number of nonzero elements in the similarity matrix, m and n are the dimensions of the similarity matrix, and F is the rank used in the factorization of the similarity matrix.

5 METAGRAPH-BASED FEATURES FUSION AND SELECTION

In this section, we describe the FM part for fusing multiple groups of metagraph based latent features. Existing HIN-based RS methods [Shi et al. 2015; Yu et al. 2014] only use a linear combination of different metapath based features and thus ignore the interactions among features. To resolve this limitation, we apply FM to capture the interactions among metagraph based latent features and non-linear interactions among features (i.e., second-order interactions) when fusing various side information in HIN. In Section 5.1, we show how FM performs prediction utilizing the metagraph based latent features. Then we introduce two regularization terms in Section 5.2, which can achieve automatic metagraph selection. In Section 5.3, we depict the objective function and propose two optimization methods for it.

5.1 Combining Latent Features with FM

In this section, we introduce our FM-based algorithm for fusing different groups of latent features. As described in Section 4.3, we obtain L groups of latent features of users and items, denoted by $\mathbf{U}^1, \mathbf{B}^1, \ldots, \mathbf{U}^L, \mathbf{B}^L$, from L metagraph based user-item similarity matrices. For a sample $\mathbf{x}^n$ in the observed ratings, i.e., a pair of user and item, denoted by $\mathbf{u}_i$ and $\mathbf{b}_j$, respectively, we concatenate all

of the corresponding user and item features from the L metagraphs:

$$\mathbf{x}^n = \big[\underbrace{\mathbf{u}_i^1, \cdots, \mathbf{u}_i^L}_{\sum_{l=1}^L F_l}, \underbrace{\mathbf{b}_j^1, \cdots, \mathbf{b}_j^L}_{\sum_{l=1}^L F_l} \big] \in \mathbb{R}^d, \tag{3}$$

where $d = 2\sum_{l=1}^L F_l$, and F_l is the rank of the factorization of the similarity matrix for the l-th metagraph obtained with (1) or (2). $\mathbf{u}_i^l$ and $\mathbf{b}_j^l$, respectively, represent user and item latent features generated from the l-th metagraph, and $\mathbf{x}^n$ is a d-dimension vector representing the feature vector of the n-th sample after concatenation.

Given all of the features in (3), the predicted rating for the sample $\mathbf{x}^n$ based on FM [Rendle 2012] is computed as follows:

$$\hat{y}^n(\mathbf{w}, \mathbf{V}) = b + \sum_{i=1}^d w_i x_i^n + \sum_{i=1}^d \sum_{j=i+1}^d \langle \mathbf{v}_i, \mathbf{v}_j \rangle x_i^n x_j^n, \tag{4}$$

where b is the global bias, and $\mathbf{w} \in \mathbb{R}^d$ represents the first-order weights of the features. $\mathbf{V} = [\mathbf{v}_i] \in \mathbb{R}^{d \times K}$ represents the second-order weights for modeling the interactions among the features, and $\mathbf{v}_i$ is the i-th row of the matrix $\mathbf{V}$, which describes the i-th variable with K factors. x_i^n is the i-th feature in $\mathbf{x}^n$. The parameters can be learned by minimizing the mean square loss:

$$\ell(\mathbf{w}, \mathbf{V}) = \frac{1}{N} \sum_{n=1}^N (y^n - \hat{y}^n(\mathbf{w}, \mathbf{V}))^2, \tag{5}$$

where y^n is an observed rating for the n-th sample, and N is the number of all observed ratings.

5.2 Metagraph Selection with Group Lasso

We need to tackle two problems when FM is applied to metagraph based latent features. The first problem is that noise may arise when there are too many metagraphs, thus impairing the predicting capability of FM. This is because not all metagraphs are useful for recommendation because the semantics captured in a metagraph may have little effect on recommendation behavior in the real world. The second problem is computational cost. All of the features are generated by MF, which means that the design matrix (i.e., features fed to FM) is dense. It increases the computational cost for learning the parameters of the model and that of online recommendation. To alleviate these two problems, we propose two novel regularization terms to automatically select useful metagraphs during training process. They can be categorized into convex and nonconvex regularizations, and either of them enables our model to automatically select useful metagraphs during the training process.

5.2.1 Convex Regularization. The convex regularizer is the $\ell_{2,1}$-norm regularization, i.e., group lasso regularization [Jacob et al. 2009], which is a feature selection method on a group of variables. Given the pre-defined non-overlapping G groups $\{\mathcal{I}_1, \ldots, \mathcal{I}_G\}$ on the parameter $\mathbf{p}$, the regularization is defined as follows.

$$\phi(\mathbf{p}) = \sum_{g=1}^G \eta_g \left\| \mathbf{p}_{\mathcal{I}_g} \right\|_2, \tag{6}$$

where $\|\cdot\|_2$ is the ℓ_2-norm, and η_g is a hyper-parameter. In our model, the groups correspond to the metagraph based features. For example, $\mathbf{U}^l$ and $\mathbf{B}^l$ are the user and item latent features generated by the l-th metagraph. For a pair of user i and item j, the latent features are $\mathbf{u}_i^l$ and $\mathbf{b}_j^l$. There are two corresponding groups of variables in $\mathbf{w}$ and $\mathbf{V}$ according to (4). Thus, with L metagraphs, $\mathbf{w}$ and $\mathbf{V}$ each has $2L$ groups of variables.

For the first-order parameters $\mathbf{w}$ in (4), which is a vector, group lasso is applied to the subset of variables in $\mathbf{w}$. Then we have:

$$\hat{\phi}(\mathbf{w}) = \sum\nolimits_{l=1}^{2L} \hat{\eta}_l \left\| \mathbf{w}^l \right\|_2, \tag{7}$$

where $\mathbf{w}^l \in \mathbb{R}^{F_l}$, which models the weights for a group of user or item features from one metagraph, and $\hat{\eta}_l$ is a hyper-parameter. For the second-order parameters $\mathbf{V}$ in (4), we have the regularizer as follows:

$$\bar{\phi}(\mathbf{V}) = \sum\nolimits_{l=1}^{2L} \bar{\eta}_l \left\| \mathbf{V}^l \right\|_F, \tag{8}$$

where $\mathbf{V}^l \in \mathbb{R}^{F_l \times K}$, the l-th block of $\mathbf{V}$ corresponds to the l-th metagraph based features in a sample, and $\|\cdot\|_F$ is the Frobenius norm.

5.2.2 Nonconvex Regularization. While convex regularizers usually make optimization easy, they often lead to biased estimation. For example, in sparse coding, the solution obtained by the ℓ_1-regularizer is often not as sparse and accurate compared to capped-ℓ_1 penalty [Zhang 2010]. Besides, in low-rank matrix learning, the estimated rank obtained with the nuclear norm regularizer is often very high [Yao et al. 2018]. To alleviate these problems, a number of nonconvex regularizers, which are variants of the convex ℓ_1-norm, have been recently proposed [Yao and Kwok 2016; Yao et al. 2018]. Empirically, these nonconvex regularizers usually outperform the convex ones. Motivated by the above observations, we propose to use nonconvex variant of (7) and (8) as follows:

$$\hat{\psi}(\mathbf{w}) = \sum\nolimits_{l=1}^{2L} \hat{\eta}_l \kappa \left(\left\| \mathbf{w}^l \right\|_2 \right), \quad \bar{\psi}(\mathbf{V}) = \sum\nolimits_{l=1}^{2L} \bar{\eta}_l \kappa \left(\left\| \mathbf{V}^l \right\|_F \right), \tag{9}$$

where κ is a nonconvex penalty function. We choose $\kappa(|\alpha|) = \log(1 + |\alpha|)$ as the log-sum-penalty (LSP) [Candès et al. 2008], since it has been shown to give the best empirical performance on learning sparse vectors [Yao and Kwok 2016] and low-rank matrices [Yao et al. 2018].

5.2.3 Comparison with Existing Methods. Yu et al. [2014] studied recommendation techniques based in HINs and applied matrix factorization to generate latent features from metapaths. Ratings are predicted using a weighted ensemble of the dot products of user and item latent features from every single metapath: $\hat{r}(\mathbf{u}_i, \mathbf{b}_j) = \sum_{l=1}^{L} \theta_l \cdot \mathbf{u}_i^l (\mathbf{b}_j^l)^\top$, where $\hat{r}(\mathbf{u}_i, \mathbf{b}_j)$ is the predicted rating for user u_i and item b_j and $\mathbf{u}_i^l$ and $\mathbf{b}_j^l$ are the latent features for u_i and item b_j from the l-th metapath, respectively. L is the number of metapaths used, and θ_l is the weight for the l-th metapath latent features. However, the predicting method is not adequate, as it fails to capture the interactions between features across different metapaths, and between features within the same metapath, resulting in a decrease of the prediction performance for all of the features. In addition, previous works on FM [Hong et al. 2013; Rendle 2012; Yan et al. 2014] only focus on the selection of one row or column of the second-order weight matrix, while $\bar{\phi}$ in our method selects a block of rows or columns (defined by metagraphs). Moreover, we are the first to adopt nonconvex regularization, i.e., $\bar{\psi}$, for weight selection in FM.

5.3 Model Optimization

Combining (5) and (9), we define our FM with Group lasso (FMG) model with the following objective function:

$$h(\mathbf{w}, \mathbf{V}) = \frac{1}{N} \sum\nolimits_{n=1}^{N} (y^n - \hat{y}^n(\mathbf{w}, \mathbf{V}))^2 + \hat{\lambda}\hat{\psi}(\mathbf{w}) + \bar{\lambda}\bar{\psi}(\mathbf{V}). \tag{10}$$

Note that when $\kappa(\alpha) = |\alpha|$ in (9), we get back (7) and (8). Thus, we directly use the nonconvex regularization in (10).

We can see that h is nonsmooth due to the use of $\hat{\phi}^{\mathbf{w}}$ and $\hat{\phi}^{\mathbf{V}}$, and nonconvex due to the nonconvexity of loss ℓ on $\mathbf{w}$ and $\mathbf{V}$. To alleviate the difficulty on optimization, inspired by [Yao and Kwok 2016], we propose to reformulate (10) as follows:

$$\bar{h}(\mathbf{w}, \mathbf{V}) = \bar{\ell}(\mathbf{w}, \mathbf{V}) + \kappa_0 \hat{\lambda} \hat{\phi}(\mathbf{w}) + \kappa_0 \bar{\lambda} \bar{\phi}(\mathbf{V}), \tag{11}$$

where $\bar{\ell}(\mathbf{w}, \mathbf{V}) = \ell(\mathbf{w}, \mathbf{V}) + g(\mathbf{w}, \mathbf{V})$, $\kappa_0 = \lim_{\beta \to 0^+} \kappa'(|\beta|)$ and

$$g(\mathbf{w}, \mathbf{V}) = \hat{\lambda} \left[\hat{\psi}(\mathbf{w}) - \kappa_0 \hat{\phi}(\mathbf{w}) \right] + \bar{\lambda} \left[\bar{\psi}(\mathbf{V}) - \kappa_0 \bar{\phi}(\mathbf{V}) \right].$$

Note that $\bar{h}$ is equivalent to h based on Proposition 2.1 in [Yao and Kwok 2016]. A very important property for the augmented loss $\bar{\ell}$ is that it is still smooth. As a result, while we are still optimizing a nonconvex regularized problem, we only need to deal with convex regularizers.

In Section 5.3.1, we show how the reformulated problem can be solved by the state-of-the-art proximal gradient algorithm [Li and Lin 2015]; moreover, such transformation enables us to design a more efficient optimization algorithm with convergence guarantee based on variance reduced methods [Xiao and Zhang 2014]. Finally, the time complexity of the proposed algorithms is analyzed in Section 5.3.3.

Remark 5.1. nmAPG was previously used in our paper [Zhao et al. 2017b]. Here, we show that it can still be applied to the new model (11). Besides, we further propose to use SVRG and show in Section 7.4.3 that it is much more efficient than nmAPG.

5.3.1 Using nmAPG Algorithm. To tackle the nonconvex nonsmooth objective function (11), we propose to adopt the PG algorithm [Parikh and Boyd 2014] and, specifically, the state-of-the-art non-monotonic accelerated proximal gradient (nmAPG) algorithm [Li and Lin 2015]. It targets at optimization problems of the form:

$$\min_{\mathbf{x}} F(\mathbf{x}) \equiv f(\mathbf{x}) + g(\mathbf{x}), \tag{12}$$

where f is a smooth (possibly nonconvex) loss function and g is a regularizer (can be nonsmooth and nonconvex). To guarantee the convergence of nmAPG, we also need $\lim_{\|\mathbf{x}\|_2 \to \infty} F(\mathbf{x}) = \infty$, $\inf_{\mathbf{x}} F(\mathbf{x}) > -\infty$, and there exists at least one solution to the proximal step, i.e., $\text{prox}_{\gamma g}(\mathbf{z}) = \arg\min_{\mathbf{x}} \frac{1}{2} \|\mathbf{x} - \mathbf{z}\|_2^2 + \gamma g(\mathbf{x})$, where $\gamma \geq 0$ is a scalar [Li and Lin 2015].

The motivation of nmAPG is two fold. First, nonsmoothness comes from the proposed regularizers, which can be efficiently handled if the corresponding proximal steps have cheap closed-form solution. Second, the acceleration technique is useful for significantly speeding up first order optimization algorithms [Li and Lin 2015; Yao and Kwok 2016; Yao et al. 2017], and nmAPG is the state-of-the-art algorithm which can deal with general nonconvex problems with sound convergence guarantee. The whole procedure is given in Algorithm 2. Note that while both $\hat{\phi}$ and $\bar{\phi}$ are nonsmooth in (11), they are imposed on $\mathbf{w}$ and $\mathbf{V}$ separately. Thus, for any $\alpha, \beta \geq 0$, we can also compute proximal operators independently for these two regularizers following [Parikh and Boyd 2014]:

$$\text{prox}_{\alpha\hat{\phi}+\beta\bar{\phi}}(\mathbf{w}, \mathbf{V}) = \left(\text{prox}_{\alpha\hat{\phi}}(\mathbf{w}), \text{prox}_{\beta\bar{\phi}}(\mathbf{V}) \right). \tag{13}$$

These are performed in steps 5 and 10 in Algorithm 2. The closed-form solution of the proximal operators can be obtained easily from Lemma 1 below. Thus, each proximal operator can be solved in one pass of all groups.

LEMMA 1 ([PARIKH AND BOYD 2014]). *The closed-form solution of $\mathbf{p}^* = prox_{\lambda\phi}(\mathbf{z})$ (ϕ is defined in (6)) is given by $\mathbf{p}^*_{I_g} = \max\left(1 - \eta_g / \left\|\mathbf{z}_{I_g}\right\|_2, 0\right) \mathbf{z}_{I_g}$ for all $g = 1, \ldots, G$.*

It is easy to verify that the above assumptions are satisfied by our objective h here. Thus, Algorithm 2 is guaranteed to produce a critical point for (11).

Algorithm 2 nmAPG algorithm for (11).

1: Initiate $\mathbf{w}_0, \mathbf{V}_0$ as Gaussian random matrices;
2: $\bar{\mathbf{w}}_1 = \mathbf{w}_1 = \mathbf{w}_0, \bar{\mathbf{V}}_1 = \mathbf{V}_1 = \mathbf{V}_0, c_1 = \bar{h}(\mathbf{w}_1, \mathbf{V}_1); q_1 = 1, \delta = 10^{-3}, a_0 = 0, a_1 = 1$, step-size α;
3: **for** $t = 1, 2, \ldots, T$ **do**
4:     $\mathbf{y}_t = \mathbf{w}_t + a_{t-1}/a_t(\bar{\mathbf{w}}_t - \mathbf{w}_t) + a_{t-1}-1/a_t(\mathbf{w}_t - \mathbf{w}_{t-1})$;
    $\mathbf{Y}_t = \mathbf{V}_t + a_{t-1}/a_t(\bar{\mathbf{V}}_t - \mathbf{V}_t) + a_{t-1}-1/a_t(\mathbf{V}_t - \mathbf{V}_{t-1})$;
5:     $\bar{\mathbf{w}}_{t+1} = \mathrm{prox}_{\alpha\kappa_0\hat{\lambda}\hat{\phi}}\left(\mathbf{w}_t - \alpha\nabla_{\mathbf{w}}\bar{\ell}(\mathbf{w}_t, \mathbf{V}_t)\right)$;
    $\bar{\mathbf{V}}_{t+1} = \mathrm{prox}_{\alpha\kappa_0\bar{\lambda}\bar{\phi}}\left(\mathbf{V}_t - \alpha\nabla_{\mathbf{V}}\bar{\ell}(\mathbf{w}_t, \mathbf{V}_t)\right)$;
6:     $\Delta_t = \|\bar{\mathbf{w}}_{t+1} - \mathbf{y}_t\|_2^2 + \|\bar{\mathbf{V}}_{t+1} - \mathbf{Y}_t\|_F^2$
7:     **if** $\bar{h}(\bar{\mathbf{w}}_{t+1}, \bar{\mathbf{V}}_{t+1}) \leq c_t - \delta\Delta_t$; **then**
8:         $\mathbf{w}_{t+1} = \bar{\mathbf{w}}_{t+1}, \mathbf{V}_{t+1} = \bar{\mathbf{V}}_{t+1}$;
9:     **else**
10:         $\hat{\mathbf{w}}_{t+1} = \mathrm{prox}_{\alpha\kappa_0\hat{\lambda}\hat{\phi}}\left(\mathbf{w}_t - \alpha\nabla_{\mathbf{w}}\bar{\ell}(\mathbf{w}_t, \mathbf{V}_t)\right)$;
        $\hat{\mathbf{V}}_{t+1} = \mathrm{prox}_{\alpha\kappa_0\bar{\lambda}\bar{\phi}}\left(\mathbf{V}_t - \alpha\nabla_{\mathbf{V}}\bar{\ell}(\mathbf{w}_t, \mathbf{V}_t)\right)$;
11:         **if** $\bar{h}(\hat{\mathbf{w}}_{t+1}, \hat{\mathbf{V}}_{t+1}) < \bar{h}(\bar{\mathbf{w}}_{t+1}, \bar{\mathbf{V}}_{t+1})$ **then**
12:             $\mathbf{w}_{t+1} = \hat{\mathbf{w}}_{t+1}, \mathbf{V}_{t+1} = \hat{\mathbf{V}}_{t+1}$;
13:         **else**
14:             $\mathbf{w}_{t+1} = \bar{\mathbf{w}}_{t+1}, \mathbf{V}_{t+1} = \bar{\mathbf{V}}_{t+1}$;
15:         **end if**
16:     **end if**
17:     $a_{t+1} = 1/2(\sqrt{4a_t^2 + 1} + 1)$;
18:     $q_{t+1} = \eta q_t + 1, c_{t+1} = 1/q_{t+1}(\eta q_t c_t + \bar{h}(\mathbf{w}_{t+1}, \mathbf{V}_{t+1}))$;
19: **end for**
20: **return** $\mathbf{w}_{T+1}, \mathbf{V}_{T+1}$.

5.3.2 Using SVRG Algorithm. While nmAPG can be an efficient algorithm for (11), it is still a batch-gradient based method, which may not be efficient when the sample size is large. In this case, the stochastic gradient descent (SGD) [Bertsekas 1999] algorithm is preferred as it can incrementally update the learning parameters. However, the gradient in SGD is very noisy. To ensure the convergence of SGD, a decreasing step size must be used, making the speed possibly even slower than batch-gradient methods.

Recently, the stochastic variance reduction gradient (SVRG) [Xiao and Zhang 2014] algorithm has been developed. It avoids diminishing step size by introducing variance reduced techniques into gradient updates. As a result, it combines the best of both worlds, i.e., incremental update of the learning parameters while keeping non-diminishing step size, to achieve significantly faster converging speed than SGD. Besides, it is also extended for the problem in (12) with nonconvex objectives [Allen-Zhu and Hazan 2016; Reddi et al. 2016]. This allows the loss function to be smooth (possibly nonconvex) but the regularizer still needs to be convex. Thus, instead of working on the original problem (10), we work on the transformed problem in (11).

To use SVRG, we first define the augmented loss for the n-th sample as $\bar{\ell}_n(\mathbf{w}, \mathbf{V}) = (y^n - \hat{y}^n(\mathbf{w}, \mathbf{V}))^2 + \frac{1}{N}g(\mathbf{w}, \mathbf{V})$. The whole procedure is depicted in Algorithm 3. A full gradient is computed in step 4, a mini-batch $\mathcal{B}$ of size m_b is constructed in step 6, and the variance reduced gradient is computed in step 7. Finally, the proximal steps can be separately executed based on (13) in step 8. As mentioned above, the nonconvex variant of SVRG [Allen-Zhu and Hazan 2016; Reddi et al. 2016]

cannot be directly applied to (10). Instead, we apply it to the transformed problem (11), where the regularizer becomes convex and the augmented loss is still smooth. Thus, Algorithm 3 is guaranteed to generate a critical point of (11).

Algorithm 3 SVRG for (11).

1: Initiate $\bar{\mathbf{w}}_0, \bar{\mathbf{V}}_0$ as Gaussian random matrices, mini-batch size m_b;
2: $\mathbf{w}_1^B = \bar{\mathbf{w}}_0, \mathbf{V}_1^B = \bar{\mathbf{V}}_0$ and step-size α;
3: **for** $t = 1, 2, \ldots, T$ **do**
4:      $\mathbf{w}_{t+1}^0 = \mathbf{w}_t^B, \mathbf{V}_{t+1}^0 = \mathbf{V}_t^B$;
5:      $\bar{\mathbf{g}}_{t+1}^{\mathbf{w}} = \nabla_{\mathbf{w}} \bar{\ell}(\bar{\mathbf{w}}_t, \bar{\mathbf{V}}_t), \bar{\mathbf{g}}_{t+1}^{\mathbf{V}} = \nabla_{\mathbf{V}} \bar{\ell}(\bar{\mathbf{w}}_t, \tilde{\mathbf{V}}_t)$;
6:      **for** $b = 0, 1, \ldots, B - 1$ **do**
7:          Uniformly randomly sample a mini-batch $\mathcal{B}$ of size m_b;
8:          $\mathbf{m}_{\mathbf{w}}^b = \frac{1}{m_b} \sum_{i_b \in \mathcal{B}} (\nabla_{\mathbf{w}} \bar{\ell}_{i_b}(\mathbf{w}_t^b, \mathbf{V}_t^b) - \nabla_{\mathbf{w}} \bar{\ell}_{i_b}(\bar{\mathbf{w}}_t, \bar{\mathbf{V}}_t)) + \bar{\mathbf{g}}_{t+1}^{\mathbf{w}}$,
           $\mathbf{m}_{\mathbf{V}}^b = \frac{1}{m_b} \sum_{i_b \in \mathcal{B}} (\nabla_{\mathbf{V}} \bar{\ell}_{i_b}(\mathbf{w}_t^b, \mathbf{V}_t^b) - \nabla_{\mathbf{V}} \bar{\ell}_{i_b}(\bar{\mathbf{w}}_t, \bar{\mathbf{V}}_t)) + \bar{\mathbf{g}}_{t+1}^{\mathbf{V}}$;
9:          $\mathbf{w}_{t+1}^{b+1} = \text{prox}_{\alpha \kappa_0 \hat{\lambda} \hat{\phi}} \left(\mathbf{w}_{t+1}^b - \alpha \mathbf{m}_{\mathbf{w}}^b \right)$,
           $\mathbf{V}_{t+1}^{b+1} = \text{prox}_{\alpha \kappa_0 \bar{\lambda} \bar{\phi}} \left(\mathbf{V}_{t+1}^b - \alpha \mathbf{m}_{\mathbf{V}}^b \right)$;
10:      **end for**
11:      $\bar{\mathbf{w}}_{t+1} = \frac{1}{B} \sum_{b=1}^{B} \mathbf{w}_{t+1}^b, \bar{\mathbf{V}}_{t+1} = \frac{1}{B} \sum_{b=1}^{B} \mathbf{V}_{t+1}^b$;
12: **end for**
13: **return** $\bar{\mathbf{w}}_{T+1}, \bar{\mathbf{V}}_{T+1}$.

5.3.3 Complexity Analysis. For nmAPG in Algorithm 2, the main computation cost is incurred in performing the proximal steps (step 5 and 10) which cost $O(NKd)$; then the evaluation of function value (step 7 and 11) costs $O(NKd)$ time. Thus, the per-iteration time complexity for Algorithm 2 is $O(NKd)$. For SVRG in Algorithm 3, the computation of the full gradient takes $O(NKd)$ in step 5; then $O(m_b BKd)$ time is needed for steps 6-10 to perform mini-batch updates. Thus, one iteration in Algorithm 2 takes $O((N + m_b B)Kd)$ time. Usually, $m_b B$ shares the same order as N [Allen-Zhu and Hazan 2016; Reddi et al. 2016; Xiao and Zhang 2014]. Thus, we set $m_b B = N$ in our experiments. As a result, SVRG needs more time to perform one iteration than nmAPG. However, due to stochastic updates, SVRG empirically converges much faster as shown in Section 7.4.3.

6 METAGRAPH BASED FEATURE FUSION WITH A HIERARCHICAL ATTENTION NETWORK

In this section, we propose a novel method based on GNN to fuse metagraph based similarities between users and items. The general idea is to treat each metagraph based similarity matrix as a new graph. Thus, the representation of each node (user/item) can be learned by adaptively aggregating neighbors' information, which is the key component of the recent Graph Neural Networks (GNN) models [Battaglia et al. 2018]. By fusing user and item embeddings from different metagraphs, a neural attention network is employed. Therefore, this proposed method is hierarchical, which is dubbed Hierarchical Attention Fusion (HAF). The architecture is given in Figure 6, which can be regarded as a neural version of the "MF + FM" framework in Figure 3, for its adoption of an end-to-end training manner based on the neural network model.

Note that the architecture of HAF is similar to HAN [Wang et al. 2019a], which is also a hierarchical attention method to learn node representation based on metapath in HIN. However, HAF is different from HAN in two aspects. First, HAF tries to learn representation for nodes of different types, i.e., users and items, while HAN is to learn representation for nodes of the same type.

Second, metagraph based similarities are used in HAF while in HAN metapath based similarities are used. In the experiments in Section 7.2, we create a variant of HAF which only utilizes metapath based similarities. Thus, it can be regarded as the application of HAN to recommendation.

To be specific, by designing L metagraphs, we can get L different user-item similarity matrices, denoted by $\mathbf{R}^1, \ldots, \mathbf{R}^L$. Following the definition in HAN [Wang et al. 2019c], we can define metagraph based neighbors in the following:

Definition 4 (Metagraph based Neighbors). Given a node i, and a metagraph M_l, the metagraph based neighbors $N^l(i)$ of the node i are defined as the set of nodes which connect to node i by instances of the metagraph M_l.

Then the L metagraph based similarity matrices can be regarded as adjacency matrices for L bipartite graphs. Thus, the metagraph based neighbors of a user are items, while the metagraph based neighbors of an item are users. We then elaborate on the technical details about HAF for the rating prediction task.
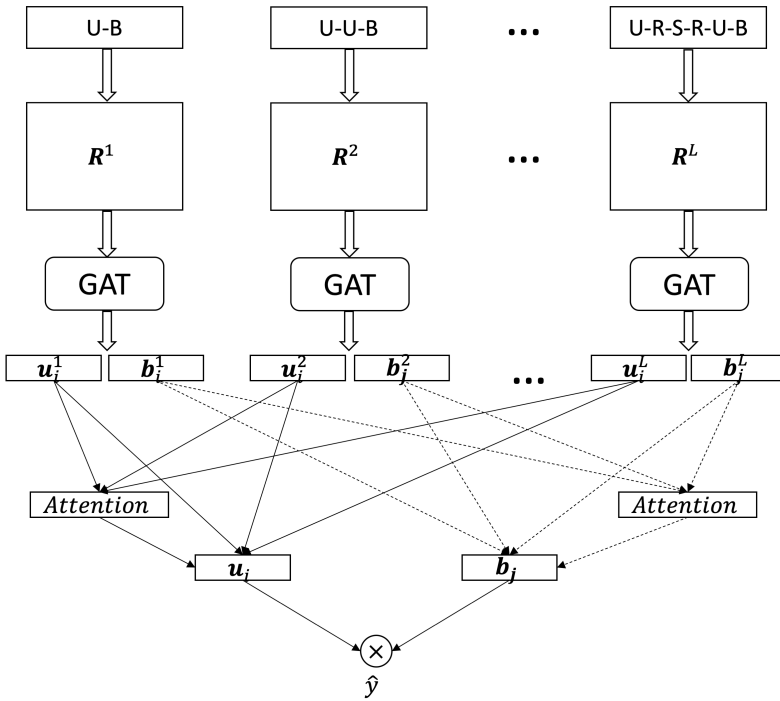

Fig. 6. HAF is a hierarchical attention model. For each metagraph based user-item similarity matrix, a multi-head GAT is applied to learning embeddings of users and items for each metagraph. To further fuse all metagraph based embeddings, a neural attentive method is introduced. Finally, the predicted rating of user i to business j is computed as the inner product of the final embeddings of $\mathbf{u}_i$ and $\mathbf{b}_j$.

6.1 Metagraph-based User and Item Embedding Learning

Since user and item are of different node types, we design type-specific encoders for users and items, respectively, which transform them into the same embedding space. To be specific, for a user i,

$$\mathbf{h}_i^l = \mathbf{W}_{\phi_i} \cdot \mathbf{e}_i^l, \tag{14}$$

where $\mathbf{e}_i^l$ and $\mathbf{h}_i^l$, respectively, are the original and transformed features of user i from the l-th bipartite graph, and $\mathbf{W}_{\phi_i}$ is the transformation matrix for user node type ϕ_i. For simplicity, we remove the superscript l when there is no misunderstanding. Since the processing of users and items are the same, we use $\mathbf{h}_j$ and $\mathbf{e}_j$ to represent the original and transformed features given an item j.

Based on Eq. (14), we can obtain L groups of transformed user and item features. Next, we show how to learn user and item representations by aggregating these transformed features following graph attention network (GAT) [Veličković et al. 2018], i.e., using the self-attention mechanism when learning user and item embeddings.

For a user-item pair (i, j) from the l-th metagraph based similarity matrix, the node-level attention, i.e., self-attention, $\mathbf{s}_{ij}$ represents the importance of item j to user i, which can be computed as $s_{ij} = Att(\mathbf{h}_i, \mathbf{h}_j)$, where Att is typically a neural network function to compute the attention coefficients. Then s_{ij} is normalized by softmax function as follows:

$$a_{ij} = \text{softmax}_j(s_{ij}) = \exp\left(\sigma(\mathbf{a}^\top \cdot [\mathbf{h}_i || \mathbf{h}_j])\right) / \sum\nolimits_{k \in N^l(i)} \exp\left(\sigma(\mathbf{a}^\top \cdot [\mathbf{h}_i || \mathbf{h}_k])\right), \qquad (15)$$

where σ is the activation function, e.g., LeakyReLU, and $||$ represents the concatenation operation. $\mathbf{a} \in \mathbb{R}^{2F}$ is the parameterized weight vector. Then the final representation of node i is computed as $\mathbf{z}_i = \sigma\left(\sum_{j \in N(i)} a_{ij} \cdot \mathbf{h}_j\right)$. Note that for simplicity, we remove the superscript of each notation, representing the corresponding metagraph, except for metagraph based neighbors $N^l(i)$.

To enhance the robustness, we use the multi-head attention, which repeats the node-level attention K times, and concatenates the learnt embeddings as the final representation:

$$\mathbf{z}_i = \overset{K}{\underset{k=1}{||}} \sigma\left(\sum\nolimits_{j \in N(i)} a_{ij} \cdot \mathbf{h}_j\right). \qquad (16)$$

Eq. (15) and (16) give the computation process for obtaining the embeddings of user i from a given megagraph M_l, and for item j, we can obtain its embeddings following the same process. Thus, for the user-item pair (i, j), we can obtain L groups of embeddings by the node-level attention, denoted as $\mathbf{u}_i^1, \cdots, \mathbf{u}_i^L, \mathbf{b}_j^1, \cdots, \mathbf{b}_j^L$.

6.2 Metagraph based User and Item Embedding Fusion

As introduced aforementioned, different metagraphs capture similarities of different semantics, and the L groups of embeddings represent different aspects of each user and item. Thus, we need to fuse all metagraph based embeddings of users and items. Intuitively, the importance of each embedding should be different for the final representation. To capture this, we further design another attention mechanism to aggregate embeddings from different metagraphs adaptively. For user i, given L groups of embeddings, $\mathbf{u}_i^1, \cdots, \mathbf{u}_i^L$, the attention is computed as

$$p_l = \frac{1}{|\mathcal{V}|} \sum\nolimits_{i \in \mathcal{V}} \mathbf{q}^\top \tanh(\mathbf{W}_u \cdot \mathbf{u}_i^l + \mathbf{b_u}), \qquad (17)$$

where $\mathbf{W}_u$ is the weight matrix, $\mathbf{b}_u$ is the bias vector, and $\mathbf{q}$ is the metagraph-level attention vector. All of the above parameters are shared for all metagraphs for meaningful comparisons. Likewise, we normalize p_l over all metagraphs by softmax function $g_l = \exp(p_l) / \sum_{l=1}^L \exp(p_l)$. With these learned attention weights, we can fuse all metagraph based embeddings to obtain the final representation for user i as follows:

$$\mathbf{u}_i = \sum\nolimits_{l=1}^L g_l \cdot \mathbf{u}_i^l.$$

The final representation for item j can be obtained in the same process, denoted as $\mathbf{b}_j$. After obtaining the final representation for user i and item j, the predicted rating is computed by dot production, $\hat{y} = \mathbf{u}_i^\top \mathbf{b}_j$. To train the whole framework, we use the mean square loss in Eq. (5) and

obtain task-specific user and item representations via back propagation under the supervision of the observed ratings.

6.3 Complexity Analysis

HAF is highly efficient since the computation of node-level and metagraph-level attention can be implemented in parallel for each node and each metagraph. Similar to GAT, the complexity of HAF is $O((|\mathcal{V}_u| + |\mathcal{V}_b|) \cdot F_e \cdot F_h \cdot K + |\mathcal{E}_{ub}| \cdot F_h \cdot K + (|\mathcal{V}_u| + |\mathcal{V}_b|) \cdot F_q \cdot F_h \cdot K)$, where $|\mathcal{V}_u|$ and $\mathcal{V}_b$ are the number of users and businesses, respectively. K is the number of heads in Eq. (16). $\mathcal{E}_{ub}$ is the number of non-zero elements in each metagraph based similarity matrix. We remove the superscript denoting the specific metagraph for simplicity, since the computation process can be executed individually. F_e, F_h, F_q are the dimension size of the vector $\mathbf{e}, \mathbf{h}, \mathbf{q}$, respectively.

7 EXPERIMENTS

In this section, we conduct extensive experiments to demonstrate the effectiveness of our proposed frameworks, including FMG and HAF. We first introduce the datasets, evaluation metrics and experimental settings in Section 7.1. In Section 7.2, we show the recommendation performance of our proposed frameworks compared to several state-of-the-art recommendation methods. We analyze the influence of the both convex and nonconvex group lasso regularization in Section 7.3. Besides the group lasso regularizers, in Section 7.4, we further analyze other important components of FMG, including the feature extraction methods in the MF part, the influence of the rank of second-order weight matrix in the FM part, and comparisons between different optimization algorithms in the FM part. Further, we give a detailed analysis of different parameters of HAF framework as well as visualize the attention weight distribution over metagraphs in Section 7.5.

7.1 Setup

To demonstrate the effectiveness of HIN for recommendation, we conduct experiments using two datasets with rich side information. The first dataset is Yelp, which is provided for the Yelp challenge.[2] Yelp is a website where a user can rate local businesses or post photos and review about them. The ratings fall in the range of 1 to 5, where higher ratings mean users like the businesses while lower rates mean users dislike business. Based on the collected information, the website can recommend businesses according to the users' preferences. The second dataset is Amazon Electronics,[3] which is provided in [He and McAuley 2016]. As we know, Amazon highly relies on RSs to present interesting items to its users. We extract subsets of entities from Yelp and Amazon to build the HINs, which include diverse types and relations. The subsets of the two datasets both include around 200,000 ratings in the user-item rating matrices. Thus, we identify them as Yelp-200K and Amazon-200K, respectively. In addition, to better compare our frameworks with existing HIN-based methods, we also use the datasets provided in the CIKM paper [Shi et al. 2015], which are denoted as CIKM-Yelp and CIKM-Douban, respectively. Note that four datasets are used to compare the recommendation performance of different methods, as shown in Section 7.2. To evaluate other aspects of our model, we only conduct experiments on the first two datasets, i.e., the Yelp-200K and Amazon-200K datasets. The statistics of our datasets are shown in Table 1. For the detailed information of CIKM-Yelp and CIKM-Douban, we refer the readers to [Shi et al. 2015].

To evaluate the recommendation performance, we adopt the root-mean-square-error (RMSE) as our metric, which is the most popular for rating prediction in the literature [Koren 2008; Ma et al. 2011; Mnih and Salakhutdinov 2007]. It is defined as RMSE = $\sqrt{\sum_{y^n \in \mathcal{R}_{test}} (y^n - \hat{y}^n)^2} / \sqrt{|\mathcal{R}_{test}|}$,

---

[2]https://www.yelp.com/dataset_challenge
[3]http://jmcauley.ucsd.edu/data/amazon/

Table 1. Statistics of the Yelp-200K and Amazon-200K datasets.

	Relations(A-B)	Number of A	Number of B	Number of (A-B)	Avg Degrees of A/B
Amazon-200K	User-Review	59,297	183,807	183,807	3.1/1
	Business-Category	20,216	682	87,587	4.3/128.4
	Business-Brand	95,33	2,015	9,533	1/4.7
	Review-Business	183,807	20,216	183,807	1/9.1
	Review-Aspect	183,807	10	796,392	4.3/79,639.2
Yelp-200K	User-Business	36,105	22,496	191,506	5.3/8.5
	User-Review	36,105	191,506	191,506	5.3/1
	User-User	17,065	17,065	140,344	8.2/8.2
	Business-Category	22,496	869	67,940	3/78.2
	Business-Star	22,496	9	22,496	1/2,499.6
	Business-State	22,496	18	22496	1/1,249.8
	Business-City	22,496	215	22,496	1/104.6
	Review-Business	191,506	22,496	191,506	1/8.5
	Review-Aspect	191,506	10	955,041	5/95,504.1

Table 2. The density of rating matrices in the four datasets (Density = $\frac{\#\text{Ratings}}{\#\text{Users} \times \#\text{Items}}$).

	Amazon-200K	Yelp-200K	CIKM-Yelp	CIKM-Douban
Density	0.015%	0.024%	0.086%	0.630%

where $\mathcal{R}_{test}$ is the set of all the test samples, $\hat{y}^n$ is the predicted rating for the n-th sample, y^n is the observed rating of the n-th sample in the test set. A smaller RMSE value means better performance.

We compare the following baseline models to our approaches.

- **RegSVD** [Paterek 2007]: The basic matrix factorization model with L_2 regularization, which uses only the user-item rating matrix. We use the implementation in [Guo et al. 2015].
- **FMR** [Rendle 2012]: The factorization machine with only the user-item rating matrix. We adopt the method in Section 4.1.1 of [Rendle 2012] to model the rating prediction task. We use the code provided by the authors.[4]
- **HeteRec** [Yu et al. 2014]: It is based on metapath based similarity between users and items. A weighted ensemble model is learned from the latent features of users and items generated by applying matrix factorization to the similarity matrices of different metapaths. We implemented it based on [Yu et al. 2014].
- **SemRec** [Shi et al. 2015]: It is a metapath based recommendation technique on weighted HIN, which is built by connecting users and items with the same ratings. Different models are learned from different metapaths, and a weight ensemble method is used to predict the users' ratings. We use the code provided by the authors.[5]
- **FMG**: The proposed framework (Figure 3) with convex group lasso regularizer in (7) and (8) used with factorization machine. The model is proposed in our previous work [Zhao et al. 2017b]; **FMG(LSP)**: Same as FMG, except nonconvex group lasso regularizer in (9) is used.
- **HAF(MP)**: the proposed hierarchical graph attention network with metapath, i.e., on Yelp, M_9 is removed, and on Amazon, M_6 is removed.
- **HAF(MG)**: the proposed hierarchical graph attention network with all metagraphs.

---

[4]http://www.libfm.org/

[5]https://github.com/zzqsmall/SemRec

Note that it is reported in [Shi et al. 2015] that SemRec outperforms the method in [Yu et al. 2013], which uses metapath based similarities as regularization terms in matrix factorization. Thus, we do not include [Yu et al. 2013] for comparison. All methods, except for HAF, are run in a server (OS: CentOS release 6.9, CPU: Intel i7-3.4GHz, RAM: 32GB). For HAF, it is run on a GPU 2080Ti (Memory: 12GB, Cuda version: 10.2). For baselines and FMG methods, they are implement with Python 2.7.5, and for HAF methods, they are implement with Pytorch (version 1.2) [Paszke et al. 2019] on top of Deep Graph Library (DGL) [Wang et al. 2019b].

On Amazon-200K and Yelp-200K datasets, we use the metagraphs in Figures 5 and 4 for HeteRec, SemRec, FMG, and FMG(LSP), while on CIKM-Yelp and CIKM-Douban, we use the metapaths provided in [Shi et al. 2015] for these four methods. To get the aspects (e.g., A in Figures 4 and 5) from review texts, we use a topic model software Gensim [Rehurek and Sojka 2010] to extract topics from the review texts and use the extracted topics as aspects. The number of topics is set to 10 empirically.

In Section 7.2, we use the four datasets in Table 2 to compare the recommendation performance of our models and the baselines. For the experimental settings, we randomly split the whole dataset into 80% for training, 10% for validation and the remaining 10% for testing. The process is repeated five times and the average RMSE of the five rounds is reported. Besides, for the parameters of our models, we set $\hat{\lambda} = \bar{\lambda} = \lambda$ in Eq. (10) for simplicity, and λ is set to obtain the optimal value on different validation datasets. As in [Zhao et al. 2017b], F and K are set to 10 for its good performance and computational efficiency. For the two variants of HAF, the hidden vector size is set to 32, the output embedding size to 32, the number of heads in self-attention part to 4, the learning rate and L_2 norm to 0.0001, the dropout is set to 0.1, and the training epochs to 200. From Sections 7.3 to Section 7.5, to explore the influences of different settings of the proposed frameworks, we create two smaller datasets, Amazon-50K and Yelp-50K, where only 50,000 ratings are randomly sampled from Amazon-200K and Yelp-200K.

7.2 Recommendation Effectiveness

The RMSEs of all methods are shown in Table 3. For CIKM-Yelp and CIKM-Douban, we directly report the performance of SemRec from [Shi et al. 2015] since the same amount of training data is used in our experiemen. Besides, the results of SemRec on Amazon-200K are not reported, as the programs crashed due to large demand of memory.

Table 3. Recommendation performance of all approaches in terms of RMSE. The lowest RMSEs (according to the pairwise t-test with 95% confidence) are highlighted.

	Amazon-200K	Yelp-200K	CIKM-Yelp	CIKM-Douban
RegSVD	2.9656±0.0008	2.5141±0.0006	1.5323±0.0011	0.7673±0.0010
FMR	1.3462±0.0007	1.7637±0.0004	1.4342±0.0009	0.7524±0.0011
HeteRec	2.5368±0.0009	2.3475±0.0005	1.4891±0.0005	0.7671±0.0008
SemRec	—	1.4603±0.0003	1.1559(*)	0.7216(*)
FMG	1.1953±0.0008	1.2583±0.0003	1.1167±0.0011	0.7023±0.0011
FMG(LSP)	1.1980±0.0010	1.2593±0.0005	1.1255±0.0012	**0.7035±0.0013**
HAF(MP)	1.1953±0.0003	1.2470±0.0008	1.1170±0.0012	0.7035±0.0017
HAF(MG)	**1.1905±0.0002**	**1.2335±0.0007**	**1.1139±0.0010**	**0.6975±0.0021**

Firstly, we can see that both FMG and FMG(LSP) consistently outperform all baselines on the four datasets. This demonstrates the effectiveness of the proposed "MF + FM" framework shown in Figure 3. Note that the performance of FMG and FMG(LSP) are very close, but FMG(LSP) needs fewer features to achieve such performance, which supports our motivation to use nonconvex

regularization for selecting features. In the following two sections, we will compare in detail the two regularizers. Besides, HAF can further decrease RMSE, which demonstrates the effectiveness of the hierarchical attention mechanism. In other words, it demonstrates the superiority of deep learning methods for HIN-based RS, which have been explored in recent works [Fan et al. 2019; Hu et al. 2018; Jin et al. 2020; Shi et al. 2019]. Note that HAF(MG) outperforms HAF(MP), thus demonstrating the importance of complex semantics captured by metagraphs, which motivates the introduction of metagraph in the conference version of this work [Zhao et al. 2017b].

Secondly, from Table 3, we can see that comparing to RegSVD and FMR, which only use the rating matrix, SemRec and FMG, which use side information from metagraphs, are significantly better. In particular, the sparser the rating matrix, the more significant is the benefit produced by the additional information. For example, on Amazon-200K, FMG outperforms RegSVD by 60%, while for CIKM-Douban, the percentage of RMSE decrease is 8.5%. Note that the performance of HeteRec is worse than FMR, despite the fact that we have tried our best to tune the model. This aligns with our discussion in Section 5 that a weighting ensemble of dot products of latent features may cause information loss among the metagraphs and fail to reduce noise caused by having too many metagraphs. These demonstrate the effectiveness of FMG for fusing various side information for recommendation.

When comparing the results of FMG and SemRec, we find that the performance gap between them are not that large, which means that SemRec is still a good method for rating prediction, especially when comparing to the other three baselines. The good performance of SemRec may be attributed to the reason that it incorporates rating values into HIN to create a weighted HIN, which can better capture the metagraph or metapath based similarities between users and items.
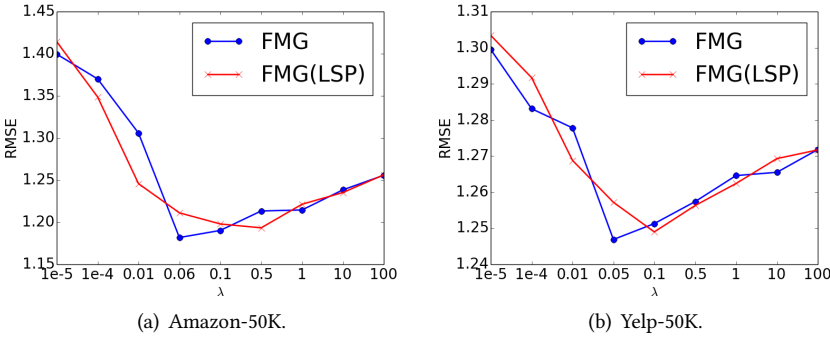

(a) Amazon-50K.   (b) Yelp-50K.

Fig. 7. RMSE v.s λ on the Amazon-50K and Yelp-50K datasets.

7.3 The Impact of Group Lasso Regularizer

In this part, we study the impact of group lasso regularizer for FMG. Specifically, we show the trend of RMSE by varying λ (with $\hat{\lambda} = \bar{\lambda} = \lambda$ in (10)), which controls the weights of group lasso. The RMSEs of Amazon-50K and Yelp-50K are shown in Figure 7(a) and (b), respectively. We can see that with λ increasing, RMSE decreases first and then increases, demonstrating that λ values that are too large or too small are not good for the performance of rating prediction. Besides, we observe that the trend of the FMG(LSP) is similar to that of FMG, except that the best performance is achieved with different λ's.

7.3.1 Sparsity of $\mathbf{w}$, $\mathbf{V}$. We study the sparsity of the learned parameters, i.e., the ratio of zeros in $\mathbf{w}$, $\mathbf{V}$, after learning. We define NNZ (number of non zeros) as $\frac{nnz}{w_n + v_n}$, where *nnz* is the total number
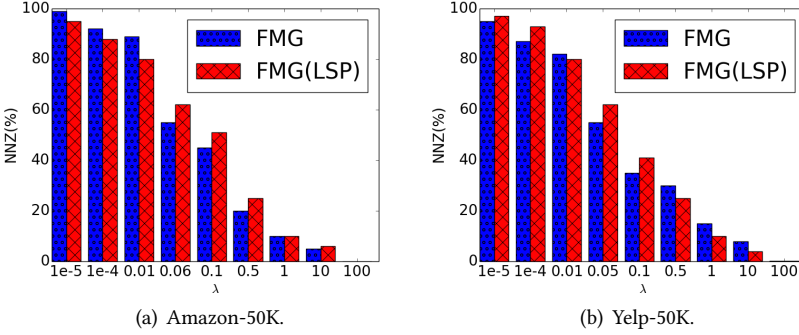
Fig. 8. The trend of NNZ by varying λ on the Amazon-50K and Yelp-50K datasets. On Amazon-50K, FMG performs best when $\lambda = 0.06$, and FMG(LSP) is the best when $\lambda = 0.5$. On Yelp-50K, FMG performs best when $\lambda = 0.05$, and FMG(LSP) best when $\lambda = 0.1$.

of nonzero elements in $\mathbf{w}$ and $\mathbf{V}$, and w_n and v_n are the number of entries in $\mathbf{w}$ and $\mathbf{V}$, respectively. The smaller NNZ, the fewer the nonzero elements in $\mathbf{w}$ and $\mathbf{V}$, and the fewer the metagraph based features left after training. The trend of NNZ with different λ's is shown in Figure 8. We can see that with λ increasing, NNZ becomes smaller, which aligns with the effect of group lasso. Note that the trend is non-monotonic due to the nonconvexity of the objective. Besides, NNZ of the parameters of FMG(LSP) is much smaller than that of FMG when the best performance on both Amazon-50K and Yelp-50K is achieved. This is due to the effect of nonconvexity of LSP, which can induce larger sparsity of the parameters with a smaller loss of performance gain.

Besides, we emphasize an interesting discovery here. From Figure 8, we can see that on both Amazon-50K and Yelp-50K the NNZ of FMG(LSP) is smaller than that of FMG when they both obtain the best performance. For example, on Amazon-50K, FMG performs best with $\lambda = 0.06$ and $NNZ = 0.52$, while FMG(LSP) performs best with $\lambda = 0.5$ and $NNZ = 0.25$. Similar cases exist on Yelp-50K. In other words, to obtain the best performance, nonconvex regularizers can induce larger sparsity, which means they can select useful features more effectively, i.e., they can achieve comparable performance with fewer selected metagraphs.

7.3.2 The Selected Metagraphs. Recall that in Eq. (4), we introduce $\mathbf{w}$ and $\mathbf{V}$, respectively, to capture the first-order weights for the features and second-order weights for interactions of the features. Thus, after training, the nonzero values in $\mathbf{w}$ and $\mathbf{V}$ represent the selected features, i.e., the selected metagraphs. We list in Table 4 the selected metagraphs corresponding to nonzero values in $\mathbf{w}$ and $\mathbf{V}$ from the perspective of both users and items, when lowest RMSEs are achieved.

Table 4. The selected metagraphs by FMG and FMG(LSP) on Amazon-50K and Yelp-50K datasets. We show the selected latent features from the perspective of users and items and from both first-order and seconder-order parameters.

		User-Part		Item-Part	
		first-order	second-order	first-order	second-order
Amazon -50K	FMG	M_1-M_3,M_5	M_1-M_6	M_2,M_3,M_5,M_6	M_2,M_5,M_6
	FMG(LSP)	M_1,M_5	-	M_2,M_5	-
Yelp -50K	FMG	M_1-M_4,M_6,M_8	M_1-M_3,M_5,M_8	M_1-M_5,M_8,M_9	M_3,M_8
	FMG(LSP)	M_1,M_3,M_4,M_8	M_2, M_3, M_8	M_1-M_5,M_8	M_8

From Table 4, for FMG, we can observe that the metagraphs with style like $U \rightarrow * \leftarrow U \rightarrow B$ are better than those like $U \rightarrow B \rightarrow * \leftarrow B$. We use $U \rightarrow * \leftarrow U \rightarrow B$ to represent metagraphs like M_2, M_3, M_8, M_9 in Figure 4 (Yelp) and M_2, M_5, M_6 in Figure 5 (Amazon), and $U \rightarrow B \rightarrow * \leftarrow B$ to represent metagraphs like M_4, M_5, M_6, M_7 in Figure 4 and M_3, M_4 in Figure 5. On Yelp-50K, we can see that metagraphs like M_2, M_3, M_8, M_9 tend to be selected while $M_4 - M_7$ are removed. This means that on Yelp, recommendations by friends or similar users are better than those by similar items. Similar observations can be made on Amazon-50K, i.e., M_3, M_4 tend to be removed. Furthermore, on both datasets, complex structures like M_9 in Figure 4 and M_6 in Figure 5 are found to be important for item latent features. This demonstrates the importance of the semantics captered by metagraphs, which are ignored in previous metapath based RSs [Shi et al. 2015; Yu et al. 2013, 2014]. The observations on FMG(LSP) are very similar to that of FMG, i.e., metagraphs with style like $U \rightarrow * \leftarrow U \rightarrow B$ are better than those like $U \rightarrow B \rightarrow * \leftarrow B$. On Yelp-50K, metagraphs like M_2, M_3, M_8 tend to be selected while $M_4 - M_7$ are removed, while on Amazon-50K M_3, M_4 tend to be removed.

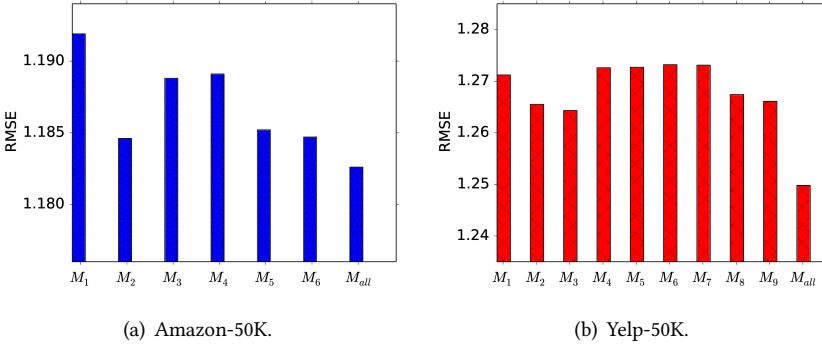(a) Amazon-50K.　　　　　　　　　　　　　(b) Yelp-50K.

Fig. 9. RMSE of each metagraph on the Amazon-50K and Yelp-50K datasets. M_{all} is our model trained with all metagraphs.

7.3.3 Performance with Single Metagraph. In this part, we compare the performance of different metagraphs separately on Amazon-50K and Yelp-50K. In the training process, we use only one metagraph for user and item features and then predict with FMG and evaluate the results obtained by the corresponding metagraph. Specifically, we run experiments to compare RMSE of each metagraph in Figures 4 and 5. The RMSE of each metagraph is shown in Figure 9. Note that we show for comparison the RMSE when all metagraphs are used, which is denoted by M_{all}.

From Figure 9, we can see that on both Amazon-50K and Yelp-50K, the performance is the best when all metagraph-based user and item features are used, which demonstrates the usefulness of the semantics captured by the designed metagraphs in Figures 4 and 5. Besides, we can see that on Yelp-50K, the performance of $M_4 - M_7$ is the worst, and on Amazon-50K, the performance of $M_3 - M_4$ is also among the worst three. Note that they are both metagraphs with style like $U \rightarrow B \rightarrow * \leftarrow B$. Thus, it aligns with the observation in the above two sections that metagraphs with style like $U \rightarrow * \leftarrow U \rightarrow B$ are better than those like $U \rightarrow B \rightarrow * \leftarrow B$. These similar observations described in these three sections can be regarded as domain knowledge, which indicates that we should design more metagraphs with style $U \rightarrow * \leftarrow U \rightarrow B$.

Finally, for M_9 on Yelp-50K and M_6 on Amazon-50K, we can see that their performance are among the best three, which demonstrates the usefulness of the complex semantics captured in M_9 on Yelp-50K and M_6 on Amazon-50K.

7.4   Analysis of Other Components of FMG

We conduct experiments to further analyze other important components of the proposed "MF + FM" framework in Figure 3, including the feature extraction methods in the MF part, the influence of the rank of second-order weight matrix in FM part, and comparisons between different optimization algorithms in the FM part.

7.4.1   Feature Extraction Methods. In this part, we compare the performance of different feature extraction methods in MF part, i.e., NNR and MF described in Section 4.2. Note that, the parameter F of MF and μ of NNR will lead to different number of latent features for different similarity matrices. Figure 10 shows the performance with different d, i.e., total length of the input features. We can see that latent features from NNR have slightly better performance than MF, while the feature dimension resulting from NNR is much larger. These observations support our motivation to use these two methods in Section 4.3, that is, NNR usually has better performance while the recovered rank is often much higher than that of MF. Thus, we can conclude that, NNR is better for extracting features, while MF is more suitable for a trade-off between performance and efficiency.
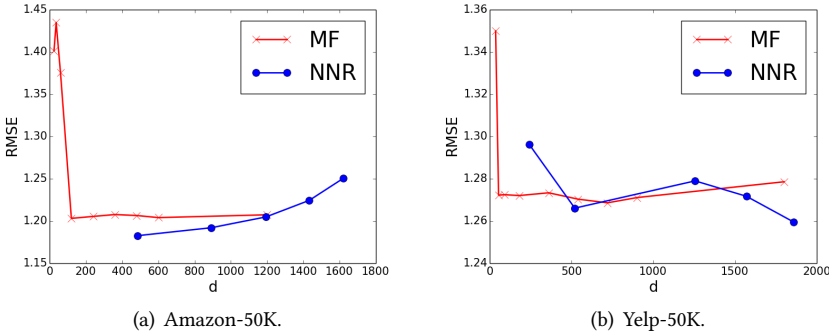

(a) Amazon-50K.   (b) Yelp-50K.

Fig. 10.   The performance of latent features obtained from MF and NNR.

7.4.2   Rank of Second-Order Weights Matrix. In this part, we show the performance trend by varying K, which is the rank of the second-order weights $\mathbf{V}$ in the FMG model (see Section 5). For the sake of efficiency, we conduct extensive experiments on Amazon-50K and Yelp-50K and employ the MF-based latent features. We set K to values in the range of $[2, 3, 5, 10, 20, 30, 40, 50, 100]$, and the results are shown in Figure 11. We can see that the performance becomes better with larger K values on both datasets and reaches a stable performance after $K = 10$. Thus, we fix $K = 10$ for all other experiments.

7.4.3   Optimization Algorithm. Here, we compare the SVRG and nmAPG algorithms proposed in Section 5.3. Besides, we also use SGD as a baseline since it is the most popular algorithm for models based on factorization machine [Hong et al. 2013; Rendle 2012]. Again, we use the Amazon-50K and Yelp-50K datasets. As suggested in [Xiao and Zhang 2014], we compare the efficiency of various algorithms based on RMSE w.r.t. the number of gradient computations divided by N.

The results are shown in Figure 12. We can observe that SGD is the slowest among all three algorithms and SVRG is the fastest. Although SGD can be faster than nmAPG at the beginning, the diminishing step size used to guarantee convergence of stochastic algorithms finally drags SGD down to become the slowest. SVRG is also a stochastic gradient method, but it avoids the problem of diminishing step size using variance reduced technique, which results in even faster speed than
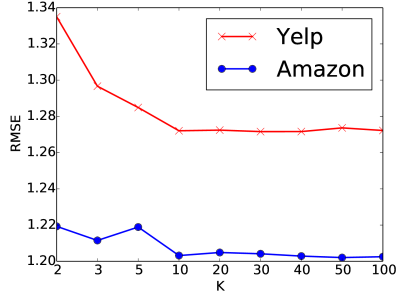
Fig. 11. The trend of RMSE of FMG w.r.t. K.

nmAPG. Finally, as both SVRG and nmAPG are guaranteed to produce a critical point of (10), they have the same empirical prediction performance. Therefore, in practice, the suggestion is to use SVRG as the solver because of the faster speed and empirically good performance.
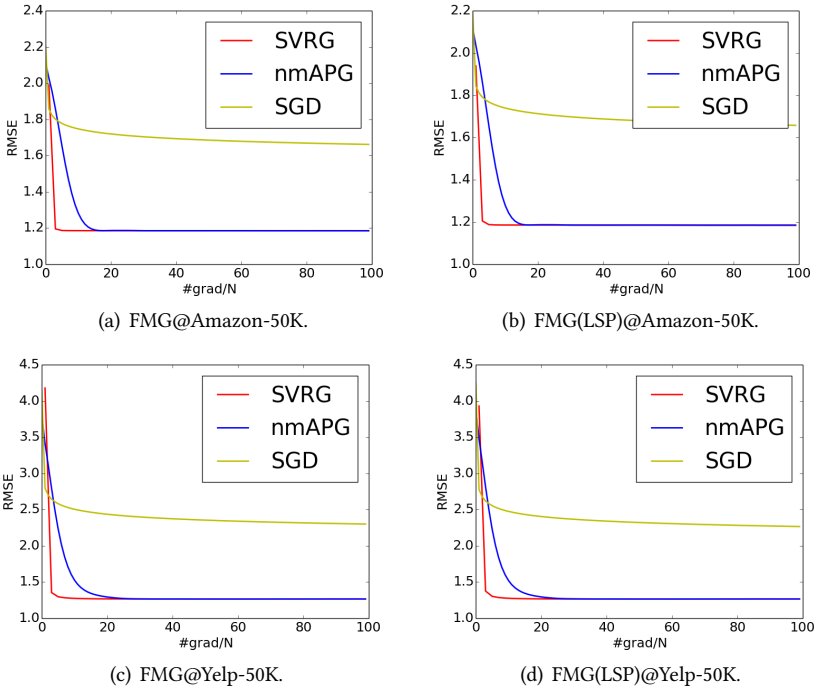

(a) FMG@Amazon-50K.

(b) FMG(LSP)@Amazon-50K.

(c) FMG@Yelp-50K.

(d) FMG(LSP)@Yelp-50K.

Fig. 12. Comparison of various algorithms on the Amazon-50K and Yelp-50K datasets.

7.5 Parameter Analysis of HAF

In this section, we conduct more experiments to show the influences of different parameters of the proposed HAF. The following three parameters are chosen: the output embedding size, the number of heads in node-level attention, and the metagraph-level attention vector size. We run the experiments with HAF by varying the corresponding parameters, and report the trend of test RMSEs. Finally, we visualize the attention weights to show the importance of each metagraph.

7.5.1   The Influence of the Output Embedding Size. The output embedding size is varied in [8, 16, 32, 64, 128, 256], and the performance trending is shown in Figure 13. We can see that with the increase of the output embedding size, the RMSE decreases firstly and then increases, which means that either too large or too small sizes of the output embedding will impair the performance. Thus, we set it to 32 in Section 7.2 according to Figure 13.
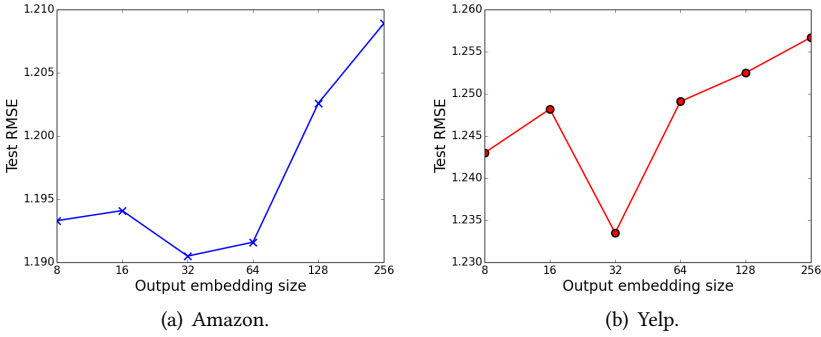

(a) Amazon.   (b) Yelp.

Fig. 13. The trend of test RMSE w.r.t the output embedding size of HAF.

(a) Amazon.   (b) Yelp.
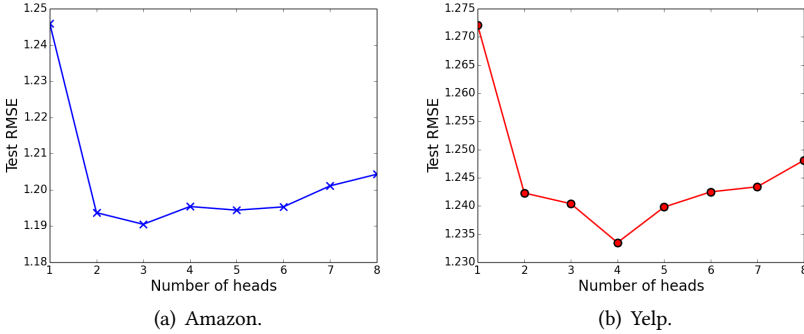
Fig. 14. The trend of test RMSE w.r.t the number of heads in node-level attention of HAF.

7.5.2   The Influence of the Number of Heads in Node-level Attention. As shown in Eq. (15), the number of heads can affect the output embedding of the node-level attention and thus the final performance. We vary the number of heads in [1, 2, 3, 4, 5, 6, 7, 8], and the performance trends are shown in Figure 14. We can see that HAF achieves the best performance when the number of heads is 3 (Amazon) or 4 (Yelp). It does not necessarily improve the performance when the number of heads is larger, which is the case in other works [Wang et al. 2019a].

7.5.3   The Influence of the Metagraph-level Attention Vector Size. The metagraph-level attention size is denoted by $\mathbf{q}$ in Eq. (17), which affects the fusion of metagraph based embeddings. The size is varied in [8, 16, 32, 64, 128, 256], and the results are shown in Figure 15. We can see that the trend is similar to that of the output embedding size, i.e., a moderate embedding size is important for the final performance.
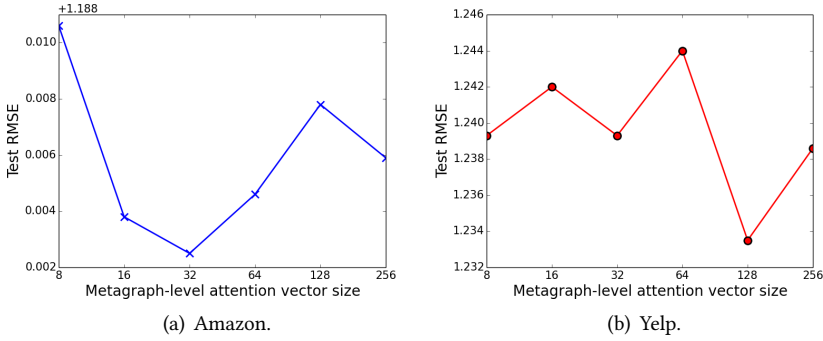
Fig. 15. The trend of test RMSE w.r.t the metagraph-level attention vector size of HAF.
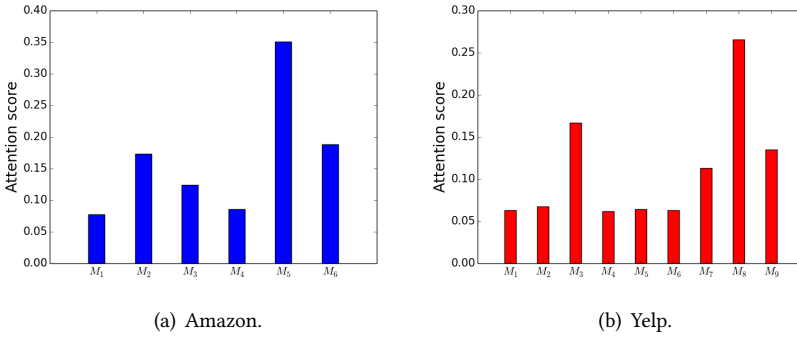

Fig. 16. The attention distribution over all metagraphs in HAF.

7.5.4   The Attention Weight Distribution. We further visualize the attention weights of different metagraphs, which are shown in Figure 16. We can see that on Amazon, M_5 is the most important, and on Yelp, M_8 is the most important. When looking at Figure 5 and 4, both of two metagraphs are $U \rightarrow R \rightarrow A \rightarrow U \rightarrow B$, which corresponds to the aspects of textual information. It might be the reason that on websites like Amazon and Yelp, the textual content plays a very important role in users' preferences and thus the recommendation performance. The metagraph-level attention can capture this pattern from the data.

8   CONCLUSION AND FUTURE WORKS

In this paper, we address the side information fusion problem in CF based recommendation scenarios over heterogeneous information networks (HIN). By using metagraphs derived given a HIN, we can capture similarities of complex semantics between users and items, based on which two fusion frameworks are proposed. The first one is the "MF + FM" framework. From each metagraph, we obtain a user-item matrix, to which we apply matrix factorization and nuclear norm regularization to obtain the user and item latent features in an unsupervised way. After that, we use a group lasso regularized factorization machine to fuse different groups of latent features extracted from different metagraphs to predict the links between users and items, i.e., to recommend items to users. The second is a deep learning model, the hierarchical attention fusion (HAF) framework, which tries to extract and fuse metagraph based latent features in an end-to-end manner. Extensive experimental results demonstrate the effectiveness of the two proposed frameworks.

In the future, we plan to explore automatic methods [Ding et al. 2020; Yao and Wang 2018; Zhao et al. 2020] to generate metagraphs instead of hand-crafting them as done in this paper. Thus, our frameworks can be quickly applied to new domains.

9 ACKNOWLEDGMENTS

REFERENCES

Z. Allen-Zhu and E. Hazan. 2016. Variance reduction for faster non-convex optimization. In *ICML*. 699–707.

Peter W Battaglia, Jessica B Hamrick, Victor Bapst, Alvaro Sanchez-Gonzalez, Vinicius Zambaldi, Mateusz Malinowski, Andrea Tacchetti, David Raposo, Adam Santoro, Ryan Faulkner, et al. 2018. Relational inductive biases, deep learning, and graph networks. *arXiv preprint arXiv:1806.01261* (2018).

D. P. Bertsekas. 1999. *Nonlinear programming.* Athena Scientific.

E. Candès and B. Recht. 2009. Exact matrix completion via convex optimization. *Foundations of Computational mathematics* 9, 6 (2009), 717.

E.J. Candès, M.B. Wakin, and S.P. Boyd. 2008. Enhancing sparsity by reweighted ℓ_1 minimization. *Journal of Fourier Analysis and Applications (JFAA)* 14, 5-6 (2008), 877–905.

Yuhui Ding, Quanming Yao, and Tong Zhang. 2020. *Propagation Model Search for Graph Neural Networks.* Technical Report.

Y. Dong, N. V Chawla, and A. Swami. 2017. metapath2vec: Scalable representation learning for heterogeneous networks. In *SIGKDD*. 135–144.

Y. Dong, Z. Hu, K. Wang, Y. Sun, and J. Tang. 2020. Heterogeneous Network Representation Learning. In *IJCAI*. 4861–4867.

S. Fan, J. Zhu, X. Han, C. Shi, L. Hu, B. Ma, and Y. Li. 2019. Metapath-guided Heterogeneous Graph Neural Network for Intent Recommendation. (2019).

Y. Fan, S. Hou, Y. Zhang, Y. Ye, and M. Abdulhayoglu. 2018a. Gotcha-Sly Malware!: Scorpion A Metagraph2vec Based Malware Detection System. In *SIGKDD*. 253–262.

Y. Fan, Y. Zhang, Y. Ye, and X. Li. 2018b. Automatic Opioid User Detection from Twitter: Transductive Ensemble Built on Different Meta-graph Based Similarities over Heterogeneous Information Network.. In *IJCAI*. 3357–3363.

Y. Fang, W. Lin, V. W. Zheng, M. Wu, J. Shi, K. Chang, and X. Li. 2019. Metagraph-based Learning on Heterogeneous Graphs. *IEEE Transactions on Knowledge and Data Engineering (TKDE)* (2019).

Y. Fang, W. Lin, W. Zheng, M. Wu, K. Chang, and X. Li. 2016. Semantic proximity search on graphs with meta graph-based learning. In *ICDE*. 277–288.

G. Guo, J. Zhang, Z. Sun, and N. Yorke-Smith. 2015. *LibRec: A Java Library for Recommender Systems.* Technical Report. School of Information Systems, Singapore Management University.

R. He and J. McAuley. 2016. Ups and downs: Modeling the visual evolution of fashion trends with one-class collaborative filtering. In *WebConf*. 507–517.

Y. He, Y. Song, J. Li, C. Ji, J. Peng, and H. Peng. 2019. HeteSpaceyWalk: a heterogeneous spacey random walk for heterogeneous information network embedding. In *CIKM*. 639–648.

J. Herlocker, J. Konstan, A. Borchers, and J. Riedl. 1999. An algorithmic framework for performing collaborative filtering. In *SIGIR*. 230–237.

L. Hong, A. S Doumith, and B. D. Davison. 2013. Co-Factorization machines: Modeling user interests and predicting individual decisions in twitter. In *WSDM*. 557–566.

S. Hou, Y. Ye, Y. Song, and M. Abdulhayoglu. 2017. HinDroid: An Intelligent Android Malware Detection System Based on Structured Heterogeneous Information Network. In *SIGKDD*. 1507–1515.

B. Hu, C. Shi, W.X. Zhao, and P. S. Yu. 2018. Leveraging Meta-path Based Context for Top- N Recommendation with A Neural Co-Attention Model. In *SIGKDD*. 1531–1540.

B. Hu, Z. Zhang, C. Shi, J. Zhou, X. Li, and Y. Qi. 2019. Cash-out User Detection based on Attributed Heterogeneous Information Network with a Hierarchical Attention Mechanism. In *AAAI*.

Z. Huang, Y. Zheng, R. Cheng, Y. Sun, N. Mamoulis, and X. Li. 2016. Meta Structure: Computing Relevance in Large Heterogeneous Information Networks. In *SIGKDD*. 1595–1604.

L. Jacob, G. Obozinski, and J. Vert. 2009. Group lasso with overlap and graph lasso. In *ICML*. 433–440.

H. Jiang, Y. Song, C. Wang, M. Zhang, and Y. Sun. 2017. Semi-supervised Learning over Heterogeneous Information Networks by Ensemble of Meta-graph Guided Random Walks. In *IJCAI*. 1944–1950.

J. Jin, J. Qin, Y. Fang, K. Du, W. Zhang, Y. Yu, Z. Zhang, and A. J Smola. 2020. An Efficient Neighborhood-based Interaction Model for Recommendation on Heterogeneous Graph. *arXiv preprint arXiv:2007.00216* (2020).

W. Kang, M. Wan, and J. McAuley. 2018. Recommendation through mixtures of heterogeneous item relationships. In *CIKM*. 1143–1152.

X. Kong, B. Cao, and P. S. Yu. 2013a. Multi-label classification by mining label and instance correlations from heterogeneous information networks. In *SIGKDD*. 614–622.

X. Kong, J. Zhang, and P. S. Yu. 2013b. Inferring anchor links across multiple heterogeneous social networks. In *CIKM*. 179–188.

Y. Koren. 2008. Factorization meets the neighborhood: a multifaceted collaborative filtering model. In *SIGKDD*. 426–434.

N. Lao and W. Cohen. 2010. Relational retrieval using a combination of path-constrained random walks. *ML* 81, 1 (2010), 53–67.

H. Li and Z. Lin. 2015. Accelerated proximal gradient methods for nonconvex programming. In *NeurIPS*. 379–387.

G. Ling, M. R. Lyu, and I. King. 2014. Ratings meet reviews, a combined approach to recommend. In *RecSys*. 105–112.

H. Ma, D. Zhou, C. Liu, M. R. Lyu, and I. King. 2011. Recommender systems with social regularization. In *WSDM*. 287–296.

J. McAuley and J. Leskovec. 2013. Hidden factors and hidden topics: Understanding rating dimensions with review text. In *RecSys*. 165–172.

A. Mnih and R. Salakhutdinov. 2007. Probabilistic matrix factorization. In *NeurIPS*. 1257–1264.

W. Pan. 2016. A survey of transfer learning for collaborative recommendation with auxiliary data. *Neurocomputing* 177 (2016), 447–453.

N. Parikh and S. Boyd. 2014. Proximal algorithms. *Foundations and Trends in Optimization* 1, 3 (2014), 127–239.

A. Paszke, S. Gross, F. Massa, A. Lerer, J. Bradbury, G. Chanan, T. Killeen, Z. Lin, N. Gimelshein, L. Antiga, et al. 2019. PyTorch: An imperative style, high-performance deep learning library. In *NeurIPS*. 8024–8035.

A. Paterek. 2007. *Improving regularized singular value decomposition for collaborative filtering*. Technical Report. Institute of Informatics, Warsaw University. 5–8 pages.

A. Pfadler, H. Zhao, J. Wang, L. Wang, P. Huang, and D.L. Lee. 2020. Billion-scale Recommendation with Heterogeneous Side Information at Taobao. In *ICDE*. 1667–1676.

S. Reddi, A. Hefny, S. Sra, B. Poczos, and A. Smola. 2016. Stochastic variance reduction for nonconvex optimization. In *ICML*. 314–323.

R. Rehurek and P. Sojka. 2010. *Software framework for topic modelling with large corpora*. Technical Report.

S. Rendle. 2012. Factorization Machines with libFM. *ACM Transactions on Intelligent Systems and Technology (TIST)* 3, 3 (2012), 57:1–57:22.

C. Shi, X. Han, S. Li, X. Wang, S. Wang, J. Du, and P.S. Yu. 2019. Deep collaborative filtering with multi-aspect information in heterogeneous networks. *IEEE Transactions on Knowledge and Data Engineering (TKDE)* (2019).

C. Shi, B. Hu, X. Zhao, and P.S. Yu. 2018. Heterogeneous Information Network Embedding for Recommendation. *IEEE Transactions on Knowledge and Data Engineering (TKDE)* (2018).

C. Shi, X. Kong, Y. Huang, Yu P. S., and B. Wu. 2014. HeteSim: A general framework for relevance measure in heterogeneous networks. *IEEE Transactions on Knowledge and Data Engineering (TKDE)* 26, 10 (2014), 2479–2492.

C. Shi, Y. Li, J. Zhang, Y. Sun, and Y. Philip. 2017. A survey of heterogeneous information network analysis. *IEEE Transactions on Knowledge and Data Engineering (TKDE)* 29, 1 (2017), 17–37.

C. Shi, Z. Zhang, P. Luo, P. S. Yu, Y. Yue, and B. Wu. 2015. Semantic path based personalized recommendation on weighted heterogeneous information networks. In *CIKM*. 453–462.

Y. Sun and J. Han. 2013. Mining heterogeneous information networks: A structural analysis approach. *ACM SIGKDD Explorations Newsletter* 14, 2 (2013), 20–28.

Y. Sun, J. Han, C. C. Aggarwal, and N. V. Chawla. 2012. When will it happen?: Relationship prediction in heterogeneous information networks. In *WSDM*. 663–672.

Y. Sun, J. Han, X. Yan, P. S. Yu, and T. Wu. 2011. PathSim: Meta path-based top-k similarity search in heterogeneous information networks. In *PVLDB*. 992–1003.

Y. Sun, B. Norick, J. Han, X. Yan, P. S. Yu, and X. Yu. 2013. PathSelClus: Integrating meta-path selection with user-guided object clustering in heterogeneous information networks. *ACM Transactions on Knowledge Discovery from Data (TKDD)* 7, 3 (2013), 11:1–11:23.

P. Veličković, G. Cucurull, A. Casanova, A. Romero, P. Lio, and Y. Bengio. 2018. Graph attention networks. *ICLR* (2018).

C. Wang, Y. Song, A. El-Kishky, D. Roth, M. Zhang, and J. Han. 2015a. Incorporating world knowledge to document clustering via heterogeneous information networks. In *SIGKDD*. 1215–1224.

C. Wang, Y. Song, H. Li, Y. Sun, Z. Zhang, and J. Han. 2017. Distant Meta-Path Similarities for Text-Based Heterogeneous Information Networks. In *CIKM*. 1629–1638.

C. Wang, Y. Song, H. Li, M. Zhang, and J. Han. 2015b. KnowSim: A Document Similarity Measure on Structured Heterogeneous Information Networks. In *ICDM*. 1015–1020.

H. Wang, F. Zhang, J. Wang, M. Zhao, W. Li, X. Xie, and M. Guo. 2019c. Exploring High-Order User Preference on the Knowledge Graph for Recommender Systems. *ACM Transactions on Information Systems (TOIS)* 37, 3 (2019), 32.

J. Wang, P. Huang, H. Zhao, Z. Zhang, B. Zhao, and D. L. Lee. 2018. Billion-scale Commodity Embedding for E-commerce Recommendation in Alibaba. In *SIGKDD*. 839–848.

M. Wang, L. Yu, D. Zheng, Q. Gan, Y. Gai, Z. Ye, M. Li, J. Zhou, Q. Huang, C. Ma, Z. Huang, Q. Guo, H. Zhang, H. Lin, J. Zhao, J. Li, A. Smola, and Z. Zhang. 2019b. *Deep Graph Library: Towards Efficient and Scalable Deep Learning on Graphs*. Technical Report.

X. Wang, H. Ji, C. Shi, B. Wang, Y. Ye, P. Cui, and P.S. Yu. 2019a. Heterogeneous graph attention network. In *WebConf*. 2022–2032.

L. Xiao and T. Zhang. 2014. A proximal stochastic gradient method with progressive variance reduction. *SIAM Journal on Optimization (SIOPT)* 24, 4 (2014), 2057–2075.

W. Xiao, H. Zhao, H. Pan, Y. Song, V. W. Zheng, and Q. Yang. 2019. Beyond Personalization: Social Content Recommendation for Creator Equality and Consumer Satisfaction. In *SIGKDD*. 235–245.

W. Xiao, H. Zhao, H. Pan, Y. Song, V. W. Zheng, and Q. Yang. 2020. Social Explorative Attention based Recommendation for Content Distribution Platforms. In *Data Mining and Knowledge Discovery (DMKD)*.

L. Yan, W. Li, G. Xue, and D. Han. 2014. Coupled group lasso for web-scale ctr prediction in display advertising. In *ICML*. 802–810.

C. Yang, Y. Feng, P. Li, Y. Shi, and J. Han. 2018. Meta-graph based hin spectral embedding: Methods, analyses, and insights. In *ICDM*. 657–666.

C. Yang, Y. Xiao, Y. Zhang, Y. Sun, and J. Han. 2020. Heterogeneous Network Representation Learning: Survey, Benchmark, Evaluation, and Beyond. *arXiv preprint arXiv:2004.00216* (2020).

Q. Yao and J. Kwok. 2015. Accelerated inexact Soft-Impute for fast large-scale matrix completion. In *IJCAI*. 4002–4008.

Q. Yao and J. Kwok. 2016. Efficient Learning with a Family of Nonconvex Regularizers by Redistributing Nonconvexity. In *ICML*. 2645–2654.

Q. Yao, J. Kwok, F. Gao, W. Chen, and T.-Y. Liu. 2017. Efficient Inexact Proximal Gradient Algorithm for Nonconvex Problems. In *IJCAI*. 3308–3314.

Q. Yao, J.T. Kwok, T. Wang, and T.Y. Liu. 2018. Large-scale low-rank matrix learning with nonconvex regularizers. *IEEE transactions on pattern analysis and machine intelligence (TPAMI)* (2018).

Q Yao and M. Wang. 2018. *Taking Human out of Learning Applications: A Survey on Automated Machine Learning*. Technical Report. arXiv preprint.

M. Ye, P. Yin, W. C. Lee, and D. L. Lee. 2011. Exploiting geographical influence for collaborative point-of-interest recommendation. In *SIGIR*. 325–334.

X. Yu, X. Ren, Q. Gu, Y. Sun, and J. Han. 2013. *Collaborative filtering with entity similarity regularization in heterogeneous information networks*. Technical Report. University of Illinois at Urbana-Champaign.

X. Yu, X. Ren, Y. Sun, Q. Gu, B. Sturt, U. Khandelwal, B. Norick, and J. Han. 2014. Personalized entity recommendation: A heterogeneous information network approach. In *WSDM*. 283–292.

D. Zhang, J. Yin, X. Zhu, and C. Zhang. 2018. Metagraph2vec: Complex semantic path augmented heterogeneous network embedding. In *PAKDD*. 196–208.

J. Zhang, P. S. Yu, and Z. Zhou. 2014. Meta-path based multi-network collective link prediction. In *SIGKDD*. 1286–1295.

T. Zhang. 2010. Analysis of multi-stage convex relaxation for sparse regularization. *Journal of Machine Learning Research (JMLR)* 11 (2010), 1081–1107.

W. Zhang, Y. Fang, Z. Liu, M. Wu, and X. Zhang. 2020. mg2vec: Learning Relationship-Preserving Heterogeneous Graph Representations via Metagraph Embedding. *IEEE Transactions on Knowledge and Data Engineering (TKDE)* (2020).

Huan Zhao, Lanning Wei, and Quanming Yao. 2020. *Simplifying Architecture Search for Graph Neural Network*. Technical Report.

H. Zhao, Q. Yao, J. Kwok, and D. Lee. 2017a. Collaborative Filtering with Social Local Models. In *ICDM*. 645–654.

H. Zhao, Q. Yao, J. Li, Y. Song, and D. Lee. 2017b. Meta-Graph Based Recommendation Fusion over Heterogeneous Information Networks. In *SIGKDD*. 635–644.

H. Zhao, Y. Zhou, Y. Song, and D.L. Lee. 2019. Motif enhanced recommendation over heterogeneous information network. In *CIKM*. 2189–2192.

V. W. Zheng, Y. Zheng, X. Xie, and Q. Yang. 2012. Towards mobile intelligence: Learning from GPS history data for collaborative recommendation. *Artificial Intelligence Journal (AIJ)* 184 (2012), 17–37.